Dynamic Econometric Testing of Climate Change and of its Causes

Travaglini, Guido

Università degli Studi di Roma "La Sapienza"

30 June 2010

Dynamic Econometric Testing of Climate Change and of its Causes

Guido Travaglini
Istituto di Economia e Finanza
Università di Roma "La Sapienza"
Email: jay_of_may@yahoo.com
June 30, 2010.

Fully revised and updated version of the paper No.669 presented at the EEA-ESEM Congress, Milan, August 27-31, 2008.

Keywords: Generalized Method of Moments, Global Warming, Principal Component and Factor Analysis, Structural Breaks.
JEL Classification: C22: Time-Series Models; C51: Model Construction and Estimation; Q54: Climate, Natural Disasters, Global Warming.

Abstract

The goal of this paper is to empirically test for structural breaks of world mean temperatures that may have ignited at some date the phenomenon known as "Climate Change" or "Global Warming". Estimation by means of the dynamic Generalized Method of Moments is conducted on a large dataset spanning the recordable period from 1850 until present, and different tests and selection procedures among competing model specifications are utilized, such as Principal Component and Principal Factor Analysis, instrument validity, overtime changes in parameters and in shares of both natural and anthropogenic forcings. The results of estimation unmistakably show no involvement of anthropogenic forcings and no occurrence of significant breaks in world mean temperatures. Hence the hypothesis of a climate change in the last 150 years, suggested by the advocates of Global Warming, is rejected. Pacific Decadal Oscillations, sunspots and the major volcanic eruptions play the lion's share in determining world temperatures, the first being a dimmer and the others substantial warmers.

1. Introduction

This paper combines several aspects of modern econometric methods: Structural Breaks Analysis (SBA), Principal Component Analysis (PCA), estimation by the Generalized Method of Moments (GMM), instrument validity and coefficient hypothesis testing in the presence of weak instruments or weak identification (WI). In particular, it develops a novel SBA method to detect level and trend breaks of time series occurring at unknown dates, it introduces a recent method based on PCA and Principal Factor Analysis (PFA) to select the true forcing regressors (henceforth defined as forcings) within a large dataset, and it utilizes several recent procedures to assess instrument validity in a context characterized by (possible) weakness and nonexogeneity.

Specifically, this composite methodology is employed at different stages of an econometric analysis of climate-related natural and anthropogenic variables that run from 1850 to present. The purpose of this methodology is to perform a series of tests regarding the timely behavior of world average temperatures during that period: the possibility of structural breaks, which is a test of the hypothesis of any significant climate change that may have occurred at some date in the past, the taxonomy of its forcings and in particular the role of anthropogenic variables, the validity (exogeneity and relevance) of the instruments utilized, the Wald-type hypothesis testing of estimated coefficients in the presence of weakness and, finally, time-varying coefficients and PCA shares of the forcings.

The plan of the paper is the following. Section 2 formulates the theoretical null and alternative hypotheses of the proposed SBA testing procedure, and empirically computes its corresponding critical values by producing their finite-sample Monte Carlo (MC) simulations. Appendix 1 contains some related off-text material on this account.

Section 3 synthetically explains the characteristics and properties of the GMM (Hansen, 1982), a classical toolkit of Instrumental Variables (IV) estimation necessary to circumvent problems arising from errors in variables, endogeneity and omitted variables. Parametric and nonparametric tests for selecting the 'best' GMM model specification among alternative sizes of the instrument and regressor sets, even in the presence of WI, are introduced and explained. Finally, its dynamic counterpart is briefly examined and a procedure for computing time-varying PCA and significance-weighted shares is introduced. Appendix 2 contains some basic information regarding the PCA and PFA procedures utilized to compute the true number of factors.

Section 4 is addressed at testing a red-hot topic that represents the center stage of many recent top-level discussions: the phenomenon known as 'Global Warming' (GW) and its anthropogenic origin, supposedly determined by the rapid pace of industrialization and the ensuing worldwide development of productive and commercial activities. The time series of world average temperatures and of a large set of human and natural forcings for the period 1850-2006 are introduced and then filtered by means of the Hodrick-Prescott (HP) procedure. After selection of the 'best' GMM model specification, dynamic GMM estimation results producing the time series of the regression coefficients, their *t* statistics and the significance-weighted shares are obtained and further examined.

Section 5 concludes by showing that there exist no significant breaks in world temperatures and that anthropogenic forcings play no role in climate changes which are instead attributable to Pacific Decadal Oscillations, sunspots and intense volcanic activity.

2. Structural Breaks Analysis (SBA)

As to the first topic considered in this paper, the literature on time-series SBA originates from Perron's seminal article (1989) that has modified for good the traditional approach of Unit Root (UR) testing (Dickey and Fuller, 1979). By departing from different null hypotheses that include UR with or without drift, trending series with I(0) or I(1) errors, with or without Additive Outliers (AO), the alternative hypotheses formulated have accordingly included different combinations that range from one single level and/or trend break (Zivot and Andrews, 1992) to multiple structural breaks of unknown date (Banerjee et al., 1992; Bai and Perron, 2003; Perron and Zhu, 2005; Perron and Yabu, 2009, Kim and Perron, 2009).

2.1. Testing for Structural Breaks: the Null and the Alternative Hypotheses

By drawing from this vast and knowledgeable experience, and especially from a chief contribution in the field (Perron and Zhu, 2005), a novel *t*-statistic testing procedure for multiple level and trend breaks occurring at unknown dates (Vogelsang, 1997) is here proposed. This procedure is easy and fast at identifying break dates, as it compares the critical *t* statistic, obtained by MC simulation under the null hypothesis of a time series with stationary noise, with the actual *t* statistic obtained under the alternative represented by a time-series model with a constant, a trend term, the two structural breaks and one or more stationary noise components.

The departing point to test for the existence of structural breaks in a time series function is the null hypothesis given by the series with I(0) errors, namely

$$1) \qquad \Delta y_t \equiv y_t - y_{t-1} = e_t$$

where y_t is nonstationary and spans the period $t \in [1,T]$, and $e_t \sim I.I.D.(0,\sigma^2)$ corresponds to a standard Data Generating Process (DGP) with draws from a random normal distribution whose underlying true process is a driftless random walk.

Let the field of fractional real numbers be $\Lambda = \{\lambda_0, 1-\lambda_0\}$, where $0 < \lambda_0 < 1$ is the preselect trimming factor, normally required to avoid endpoint spurious estimation in the presence of unknown-date breaks (Andrews, 1993). Let the true break fraction be $\lambda \in \Lambda$ for $0 < \lambda_0 < \lambda < (1-\lambda_0)$ and $\lambda_0 T \leq \lambda T \leq (1-\lambda_0)T$ the field of integers wherein the true break date occurs.

Given the null hypothesis of eq. (1), the simplest available alternative is provided by a series with a constant and a trend, their respective breaks, and a time vector of noise. Specifically, the alternative is represented by an augmented AO model (Perron, 1997), usually estimated by Ordinary Least Squares (OLS). In Sect. 3.1, the alternative will be augmented with a vector of exogenous I(0) series and estimated by GMM in order to account for heteroskedasticity, autocorrelation and endogeneity.

Formally, the alternative specification of eq. (1) is represented by a extension of the null that includes a set of deterministic variables, namely, a constant, a linear trend and their corresponding SB dummies. The result is

$$2) \qquad \Delta y_t = \mu_1(\lambda) + \mu_2(\lambda) DU_t(\lambda) + \tau_1(\lambda) t + \tau_2(\lambda) DT_t(\lambda) + \varepsilon_t(\lambda); \ \forall \lambda \in \Lambda$$

where the λ notation refers to the time-changing coefficients and variables of the dynamic equation estimation.

The disturbance $\varepsilon_t(\lambda) = I.I.D.(0,\sigma^2)$ is I(0) with $E(\varepsilon_t(\lambda)' \varepsilon_s(\lambda)) = 0; \ \forall t,s, \ s \neq t$ (Perron and Zhu, 2005; Perron and Yabu, 2009). Thus, eq. (2) is expected to be stationary and to exhibit no autocorrelation.

Specifically, the two differently defined unknown-date break dummies included in eq. (2) DU_t and DT_t are defined as follows:

A) $DU_t = 1(t > TB_t)$, a change in the intercept of Δy_t, $(\mu_1 - \mu_0)$, namely a break in the mean level of Δy_t;

B) $DT_t = (t - TB_t)1(t > TB_t)$, a change in the trend slope $(\tau_1 - \tau_0)$, namely a change in the inclination of Δy_t around the deterministic time trend.

By stacking for $t \in [1,T]$ both dummy series, we obtain the following $T \times T$ matrices:

$$\mathbf{DU} = \begin{bmatrix} 0 & 1 & 1 & ... & 1 \\ 0 & 0 & 1 & ... & 1 \\ ... & ... & ... & ... & ... \\ 0 & 0 & 0 & ... & 1 \end{bmatrix}, \qquad \mathbf{DT} = \begin{bmatrix} 0 & 1 & 2 & ... & T-1 \\ 0 & 0 & 1 & ... & T-2 \\ ... & ... & ... & ... & ... \\ 0 & 0 & 0 & ... & T-T \end{bmatrix}$$

where each row of $\mathbf{DU}$ and $\mathbf{DT}$ respectively represents DU_t and DT_t, $\forall t \in [1,T]$. The trimming factor, usually set to 10-15%, is made compulsory by the existence of zeros in both matrices that causes spurious regression estimates. Theoretically, since unknown-date structural breaks are a nuisance in regression analysis (this is not the case of standard dummies), endpoint loss of power against alternatives occurs (Andrews, 1993) because of the trailing zeros in **DU** and **DT**. In practice, however, the endpoint cuts can be asymmetric and endogenously computed by simply detecting the length of both trailing zero sets. Fortunately enough, in most cases, the trimming factor is found to be much shorter at the end of the sample, thereby letting room for the inclusion and evaluation of more recent data. For expositional simplicity, however, the notation λ_0 valid for both endpoints is retained in the present context.

The coefficients μ_0 and τ_0 are the respective pre-change values. As a general rule there follows, from the above notation, that any of the two structural breaks is represented by a vector of integers $\forall\ TB_t \in \{\lambda_0 T, (1-\lambda_0)T\}$ (Banerjee et al., 1992). From eqs. (1) and (2), $E(\Delta y_t) \equiv 0$ and $E(\mu_1 - \mu_0, \tau_1 - \tau_0)(\lambda) = 0$, that is, breaks in mean and in trend slope are a temporary phenomenon. Therefore, case A corresponds to unknown-date structural breaks in terms of temporary change(s) in the level of the endogenous variable (the "crash" model). Similarly, case B corresponds to temporary shifts in its trend slope (the "changing growth" model) (Perron 1997; Banerjee et al., 1992; Vogelsang and Perron, 1998). Eq. (2), by using both cases together, is defined by Perron and Zhu (2005) as a "local disjoint broken trend" model with I(0) errors (their "Model IIb").

In addition, for $E(\Delta y_t) \equiv 0$ in eq. (2), $E(\mu_1(\lambda), \tau_1(\lambda)) \neq 0$, i.e. the coefficients are expected not to equal zero. Appendix 1 demonstrates that β_0 holds only for a non-breaks alternative model, namely, when $\lambda = 1$. If this is not the case, i.e. when time series are characterized by a broken trend, both breaks are likely to occur.

As usual in the break literature, eq. (2) is estimated sequentially for all $\lambda \in \Lambda$. After dropping the λ notation for ease of reading from the single coefficients, we obtain a time series of length $1 + (1-\lambda_0)T$ of the coefficient vector $\hat{\beta}(\lambda) \equiv [\mu_1, \mu_2, \tau_1, \tau_2]$ which is closely akin to the Kalman filter 'changing coefficients' procedure. As a by-product, the *t* statistics of $\hat{\beta}(\lambda)$ for the same trimmed interval are obtained and defined as $\hat{t}_\mu(\lambda)_t$ and $\hat{t}_\tau(\lambda)_t$, respectively. They are nonstandard-distributed since the corresponding breaks are associated to unknown dates and thus appear as a nuisance in eq. (2), (Andrews, 1993; Vogelsang, 1999).

These *t* statistics can be exploited to separately detect time breaks of type A and/or of type B, just as with the nonstandard F, Wald, Lagrange and Likelihood Ratio tests for single breaks (Andrews, 1993; Vogelsang, 1997, 1999; Hansen, 2000) and for multiple breaks (Bai and Perron, 2003). However, different from these methods that identify the break(s) when a supremum or weighted average is achieved and tested for (e.g. Andrews, 1993), all that is required is to sequentially find as many t statistics that exceed in absolute terms the appropriately tabulated critical value for a preselect magnitude of λ.

In practice, after producing the critical values for different magnitudes of λ by MC simulation, respectively denoted as $t_T(\lambda, L)$ and $t_T(\lambda, T)$, any $n \geq 1$ occurrence for a given confidence level (e.g. 95%) whereby $\left|\hat{t}_\mu(\lambda)_t\right| > t_T(\lambda, L)$ and $\left|\hat{t}_\tau(\lambda)_t\right| > t_T(\lambda, T)$ indicates the existence of $n \geq 1$ level and trend breaks, respectively, just as with standard t-statistic testing[1].

2.2. Theoretical and Finite-sample Critical *t* Statistics

To achieve the above-stated goal, some additional notation is required. Let the K_1-sized vector of the deterministic variables of eq. (2) be specified as $X_t = \left[1, t, DU_t(\lambda), DT_t(\lambda)\right]$, and let the Ordinary Least Squares (OLS) estimated coefficient vector be

$$3) \qquad \hat{\beta}(\lambda) = \sum_{t=\lambda_0 T}^{(1-\lambda_0)T} \Delta y_t X_t \Bigg/ \sum_{t=\lambda_0}^{(1-\lambda_0)T} X_t{}' X_t$$

with variance $\sigma^2 \mathrm{I}_{K_1} \left(\sum_{t=\lambda_0}^{(1-\lambda_0)T} X_t{}' X_t \right)^{-1}$, where I_{K_1} is the $K_1 \times K_1$ identity matrix. Let also the estimated and the true parameter vectors be formally defined as $\hat{\beta}(\lambda) \equiv \left[\hat{\mu}_1, \hat{\tau}_1, \hat{\mu}_2, \hat{\tau}_2\right]$ and $\beta^* \equiv \left[\mu_1^*, \tau_1^*, \mu_2^*, \tau_2^*\right]$, respectively, such that the scaling matrix of the different rates of convergence of $\hat{\beta}(\lambda)$ with respect to β^* is given by $\Upsilon_t = diag\left[T^{1/2}, T^{3/2}, T^{1/2}, T^{3/2}\right]$ which ensures the asymptotics of the estimated parameters.

Then, by generating Δy_t according to eq. (1) we have, for $0 < \lambda < 1$

$$4) \qquad \Upsilon_T\left[\hat{\beta}(\lambda) - \beta^*\right] \xrightarrow{L} \left(\Theta_T(\lambda)\right)^{-1} \Psi_T(\lambda),$$

whereby, for $W(r)$ a standard Brownian motion in the plane $r \in [0,1]$, the following expressions ensue:

$$5) \qquad \Psi_T(\lambda) = \sigma\left[W(1), W(1) - \int_0^1 W(r)dr, (1-\lambda)W(1), (1-\lambda)\left(W(1) - \int_0^1 W(r)dr\right)\right]$$

and

$$6) \qquad \Theta_T(\lambda) = \begin{bmatrix} 1 & 1/2 & 1-\lambda & \dfrac{(1-\lambda)^2}{2} \\ & 1/3 & \dfrac{(1-\lambda^2)}{2} & \dfrac{(2-3\lambda+\lambda^3)}{6} \\ & & 1-\lambda & \dfrac{(1-\lambda)^2}{2} \\ & & & \dfrac{(1-\lambda)^3}{3} \end{bmatrix}.$$

The elements of eqs. (5) and (6) are explained in detail in Appendix 1. From eqs. (4) to (6) the limit distribution of the coefficient vector is the same as that reported by Perron and Zhu for Model IIb (2005, p.81) for a given break date, namely

$$7)\qquad \Upsilon_T\left[\hat{\beta}(\lambda)-\beta^*\right] \sim \mathrm{N}\left(\begin{bmatrix}0\\0\\0\\0\end{bmatrix}, \sigma^2\begin{bmatrix}\frac{4}{\lambda} & -\frac{6}{\lambda^2} & \frac{2}{\lambda} & \frac{6}{\lambda^2}\\ & \frac{12}{\lambda^3} & -\frac{6}{\lambda^2} & -\frac{12}{\lambda^3}\\ & & \frac{4}{\lambda(1-\lambda)} & 6\frac{2\lambda-1}{\lambda^2(1-\lambda)^2}\\ & & & 12\frac{3\lambda^2-3\lambda+1}{\lambda^3(1-\lambda)^3}\end{bmatrix}\right)$$

where the square matrix corresponds to $\left(\Theta_T(\lambda)\right)^{-1}$.

The corresponding asymptotic t statistics of the coefficient vector for testing the null hypothesis that $\hat{\beta}(\lambda)-\beta^*=0$ are computed as follows:

$$8)\qquad t_T(\lambda)=\left(\Theta_T(\lambda)\right)^{-1}\Psi_T(\lambda)\big/\left(\Omega_T(\lambda)\right)^{1/2}$$

where $\Omega_T(\lambda)=\sigma^2\mathrm{I}_4\left(\Theta_T(\lambda)\right)^{-1}$. The ensuing theoretical t statistic values regarding the level break $t_T(\lambda,L)$ and the trend break $t_T(\lambda,T)$ are thus

$$8.1)\qquad t_T(\lambda,L)=3\frac{\lambda W(1)-\int_0^1 W(r)dr}{\left[\lambda(1-\lambda)\right]^{1/2}}$$

$$8.2)\qquad t_T(\lambda,T)=3^{1/2}\frac{\lambda(3\lambda-1)W(1)-2(2\lambda-1)\int_0^1 W(r)dr}{\left[\lambda(1-\lambda)(3\lambda^2-3\lambda+1)\right]^{1/2}}$$

while the other two non-break statistics are reported in Appendix 1. The empirical critical values of the above-shown t statistics are obtained by MC simulation of the values of the null provided by eq. (1)[2]. For select magnitudes of λ running from 0.10 to 0.90, and for a reasonable sample size (T = 200), the 1%, 5% and 10% finite-sample absolute critical values of eqs. (8.1) and (8.2) are reported in Table 1 together with their 10% upper and lower confidence bands.

The critical values, after selecting the sample size and the number of draws (N=1,000), are obtained by means of the following steps:

(i) computing a $T\times T$ matrix of the standard Gaussian random variates $w_j \sim N.I.D.\left(0,v_j/\sqrt{T}\right)$, where $v_j \sim N(0,1)$, $j\in[1,T]$;

(*ii*) computing each value of e_t in eq. (1) as the algebraic sum of each column of the random variate matrix. Therefore $e_t=\sum_{j=1}^{T} w_j$ is a $T\times 1$-sized matrix of artificial discrete realizations;

(*iii*) integrating e_t over the time span $t=1,...,T$ by computing the rolling partial sums of e_t and obtain the $T\times 1$-sized matrix of nonstationary series y_t;

(*iv*) exploiting the values e_t and y_{t-1} to approximate the scalar-sized Brownian functionals $W(1)$ and $\int_0^1 W(r)dr$ of eq. (5) with the corresponding discrete sums exhibited in Appendix 1;

(*v*) repeating all of the foregoing steps N times to obtain $N\times 1$-sized vectors of functionals, and finally computing eqs. (8.1) and (8.2)[3].

From Table 1 the absolute critical values can be seen to achieve minimal absolutes at λ=0.50 and larger values at both ends of λ. Finally, except for λ=0.50, $t_T(\lambda, L)$ is smaller than $t_T(\lambda, T)$ by a factor that reaches 1.2 at both ends[4]. In addition, the reported *t* statistics are nonstandard. In fact, though exhibiting zero mean, they have non-unit variances that strictly hinge on the values of λ and of σ. As shown in Appendix 1, this is applicable also to the other two non-break statistics.

Descriptive statistics of the *t* statistic of a break in level, eq. (8.1), and of the *t* statistic of a break in trend, eq. (8.2) for 1,000 MC draws of eq. (1) for a sample size *T*=200 and break fractions $0.10 \le \lambda \le 0.90$ are supplied in Table 2. As expected, the means hover around zero for any value of λ, while the variances attain a minimal value in correspondence of λ=0.50, where they share an almost equal value and then increase by eight and ten times at both ends, respectively. Specifically, the estimated variance of the first statistic is on average 40% smaller than the second, reflecting the similar gap in their critical values reported in Table 1. Similar gaps are recorded also for the extrema and for the 1% and 99% fractile values.

3. The Generalized Method of Moments (GMM)

The time series of length $1+(1-\lambda_0)T$ of the coefficients and of the *t*-statistics may be estimated sequentially by means of GMM which exhibits the following characteristics:

1) the model used by the GMM method perfectly suits eq. (2) so that the estimated relevant *t* statistics are easily comparable to their simulated critical values of Table 1;

2) the estimated coefficients are scale-free relative to equations in levels as the regressors in origin are often differently indexed with the risk of producing, otherwise, spurious coefficient results;

3) the autocorrelation and heteroskedasticity of the error term are corrected for by using the Heteroskedasticity and Autocorrelation Consistent (HAC) covariance estimator (Newey and West, 1987);

4) By accordingly selecting the optimal instrument vector, GMM disposes of parameter inconsistency deriving from left-out variables, errors in variables (i.e. mismeasurement) and/or endogeneity.

In addition, the GMM method may be exploited to compute time-varying standard and significance-weighted PCA shares, a useful tool to assess the relevance of the regressors in determining the causative behavior of the endogenous variable. By including time changes in the parameters of eq. (2), the method is more properly defined as Dynamic GMM. This technique is described in detail in Sect. 3.2.

3.1. Properties of the GMM Estimator and Weak Instruments Robust Testing

Before delving into the dynamic version of the GMM method, some aspects of the static standard GMM estimation method must be introduced. GMM uses sample moments derived from first-stage (possibly consistent) IV estimation, usually Two-Stage Least Squares (TSLS). In turn, IV estimation requires an appropriate model setting where the major features tying the endogenous variable, the regressors and the instruments are explicitly formalized.

The departing point to construct the GMM model is represented by eq. (2) which, for ease of reading and of treatment, is simplified by removing the dynamic λ notation from therein in order to operate in a static environment. In addition, the X_t vector of deterministics of Sect. 2.2 may be made to include without any loss of generality, if desired, additional nondeterministic explanatory variables. Consider a K_2-sized vector of stationary stochastic components $\tilde{X}_t = \left[\tilde{x}_{t,1}, ..., \tilde{x}_{t,K_2}\right]$

which extends the vector of regressors to a *K*-sized vector $\mathrm{X}_t \equiv \left[X_t \vdots \tilde{X}_t \right]$, where $K = K_1 + K_2$. Therefore, the IV setup is represented by a standard structural form and its reduced-form counterpart

9.1) $$\Delta y_t = \mathrm{X}_t \beta + e_t$$

9.2) $$X_t = Z_t \Pi + v_t$$

where $\mathrm{X}_t : (T \times K)$ is defined as above, $Z_t : (T \times L)$ is a matrix of $L \geq K$ instrumental variables, $\beta : (K \times 1)$ and $\Pi : (L \times K)$ are a coefficient vector and matrix, respectively, $e_t : (T \times 1) \sim N.I.D.(0, \sigma_e^2)$ and $v_t : (T \times K) \sim N.I.D.(0, \Sigma)$ are the disturbance terms, and $E(\mathrm{X}_t ' e_t) = 0$, $E(e_t ' v_t) = 0$, $E(X_t ' Z_t) \neq 0$ and finally Π is of full rank[5].

The requirement of stationarity of eqs. (9.1) and (9.2) is crucial. In fact, nonstationary series unless cointegrated notoriously produce spurious coefficient *t* statistics, error autocorrelation and a bloated R^2 (Granger and Newbold, 1974; Phillips, 1986). Spuriousness is also found between series generated as independent stationary series with or without linear trends and with seasonality (Granger et al., 2001) or with structural breaks (Noriega and Ventosa-Santaulària, 2005). These occurrences are found in this literature with OLS regressions where the *t* statistics – in particular those of the deterministic components – diverge as the number of observations gets large[6], although HAC-based correction methods are available (Sun, 2004).

In practice, the requirements that $e_t = I.I.D.(0, \sigma_e^2)$, $\mathrm{E}(e_t ' e_s) = 0,\ t \neq s$ and also, given *p* a preselect lag integer, $\mathrm{E}\left(\sum_{i=1}^{p} e_{t-i}^2 \right) = 0$ for no heteroskedasticity must be met as from eq. (9.1). Tests to check for such occurrences are available in great numbers and kinds, e.g. the Durbin-Watson and the Breusch–Godfrey statistics, the ARCH test for heteroskedasticity, etc., and may be exploited to perform first-hand model selection. First differencing, centering-and-scaling and Hodrick-Prescott (HP) smoothed filtering (Hodrick and Prescott, 1997) are the major competitors addressed at performing the necessary data transformation to attain a stationary environment.

Recently, standard two-step GMM has undergone mounting criticism on accounts of parameter consistency and HAC optimal bandwidth selection in a small-sample setting, and especially in the presence of (many) WI (e.g. Newey and Smith, 2004; Sun et al., 2008; Newey and Windmeijer, 2009). It has been in fact demonstrated that the efficiency of the IV and of the GMM estimators can be improved by using a large instrument set at the cost – however – of heavy biases. This occurs especially in the presence of WI, which distorts standard parameter Wald-based test results culminating in the "weak IV asymptotics" in which the coefficient vector in the first-stage regression shrinks to zero as the sample size goes to infinity (Staiger and Stock, 1997; Stock and Wright, 2000; Andrews and Stock, 2007).

The Wald-type hypothesis testing considered is framed as the standard null, namely $H_0 : \beta = \beta_0$, where β_0 is some theoretical value, or the first-stage estimated coefficient (β_{TSLS}), or even zero for the entire *K*-sized coefficient vector or for an *R*-sized subset thereof $(1 \leq R < K)$. In the presence of WI such tests are found to be heavily distorted and characterized by low power. Moreover, in the many-WI case, GMM estimates are biased toward OLS estimates (Newey and Windmeijer, 2009), while the *J* test statistic of overidentifying restrictions (Hansen, 1982) has low power and produces spurious identification results (Kleibergen and Mavroeidis, 2009).

In turn, tests for detecting WI are renowned (Cragg and Donald, 1993; Stock and Yogo, 2003) and remedies are feasible by selecting the appropriate instruments, although in many empirical cases a full set of strong instruments may be unavailable[7]. Elsewise, as Yogo correctly points out (2004), researchers may be still interested at parameter estimation even in the presence of a detected WI, and size-robust parameter tests for a given null hypothesis may be employed and confidence intervals (CI) may be constructed by "inversion" of the appropriately supplied non-Wald test statistics (Moreira, 2003; Cruz and Moreira, 2005; Andrews et al. 2006; Kleibergen, 2002, 2005, 2008; Kleibergen and Mavroeidis, 2009).

The tests proposed by the mentioned authors are intended to replace the traditional testing methodology that depends on nuisance parameters (e.g. the reduced-form coefficients of eq. (9.2)). To eliminate these effects, the mentioned authors have devised these novel test statistics that are pivotal, invariant and similar[8] and thus have good size properties under both strong and WI, although not all have optimal power properties and in several cases CI might not even be constructed.

The proposed tests belong to the classes of the Anderson-Rubin (AR, Anderson and Rubin, 1949), of the score Lagrange Multiplier (LM) and of the Likelihood-Ratio (LR) test statistics. These tests originate in the field of IV estimation test (Stock and Wright, 2000; Stock et al., 2002; Stock and Yogo, 2003; Moreira, 2003) but have been recently extended to GMM (Kleibergen, 2005; Kleibergen and Mavroeidis, 2009). For ease of space, only these versions are reported in the present context, together with the corrected *J* test statistic for overidentification and the Jacobian rank statistic. They are denoted by the authors respectively as: S, KLM, MQLR, JKLM and RK, and fully described in Kleibergen (2005) and in Kleibergen and Mavroeidis (2009). Under the null they are all distributed as a χ^2 statistic with (L-K+R), R, R, (L-K) and (L-K) degrees of freedom, respectively.

The first three GMM-based statistics behave much as their IV counterparts and are similarly constructed, although with some specific differences (Kleibergen, 2005; Kleibergen and Mavroeidis, 2009). For instance, the S statistic is different from the AR test (Stock and Wright, 2000; Stock et al., 2002; Stock and Yogo, 2003) since it is represented by the value function of the Continuous Updating Estimator (CUE) (Hansen et al., 1996), but it shares with AR the asymptotic distribution which does not depend on nuisance parameters even when the instruments are arbitrarily weak. Therefore, S is pivotal and can be used for inference and for constructing valid confidence sets (i.e. CI) by inversion as with the AR statistic (Staiger and Stock, 1997). However, it has however low power under overidentification and is outperformed by KLM and MQLR, and especially by the latter (Andrews et al., 2006).

The KLM test relies on the independence between average moments and their first derivatives (the Jacobian matrix), since correlation among them is a major source of bias in conventional GMM estimates and test statistics (Newey and Smith, 2004; Kleibergen, 2005; Newey and Windmeijer, 2009)[9]. However, this test statistic exhibits a loss of power when the objective function is maximal and becomes spurious. It is also size-distorted when such correlation is high (Kleibergen and Mavroeidis, 2009).

MQLR is an extension of the Conditional LR test (Moreira, 2003), so defined because it is conditioned on a statistic that is complete and sufficient under the null hypothesis. MQLR has the desirable features of having size that is robust to many WI and near-optimal power properties with Gaussian errors, and dominates the power of both S and KLM (Andrews et al., 2006; Mikusheva, 2007). This occurs because MQLR supersedes the assumption of full-column rank of the Jacobian matrix (Sect. 3.1) and conditions the LR statistic on a matrix reduced-rank test (Kleibergen, 2005; Kleibergen and Paap, 2007).

The conditioning statistic of MQLR is RK, a statistic that tests the rank of the Jacobian under the null hypothesis and is the analog of the Cragg-Donald statistic used in IV. It is a measure of the identification of β and can be used as a pretest statistic in its own right. When β is not well identified, RK is small and by consequence the bounding distribution of MQLR is similar to that of S, but when β is well identified, RK is large and the bounding distribution of MQLR is similar to that of KLM. Finally, JKLM is a *J* statistic evaluated at the null hypothesis of zero coefficient(s), and is different from Hansen's *J* statistic, which is evaluated at the parameter estimate. It is given by S-KLM, namely, the difference between a value function and an asymptotically independent test of the validity of the moment conditions.

3.2. Parametric and Nonparametric Tests for the Selection of Alternative GMM Models

In addition to appropriate data filtering required to remove spuriousness, and to due consideration of the possible WI phenomenon, GMM modeling involves a large variety of choices regarding the size of the regressor and instrument sets (given $L \geq K$) and the magnitude of the bandwidth of the HAC weight matrix of eq. (16). Coefficient estimates and their efficiency and significance can in fact be very sensitive to different specification choices even with contiguous indicators (Hansen and West, 2002). Pretesting is thus necessary and (hopefully) sufficient to extract the "best" GMM model among different specifications, characterized each by different regressor and instrument vector sizes, HAC bandwidths and instrument strengths.

A complete although not exhaustive package of such pretest procedures contemplates three categories to be sequentially implemented for each select specification: true factor number and shares, first-stage tests, GMM tests. These categories constitute the following list:

A) True number of factors (Bai and Ng, 2002, 2007) and total number of instruments;
B) Nominal factor shares;
C) First-stage tests for endogeneity: one-lag Granger causality F statistics running from structural residuals in eq. (9.1) to forcings and viceversa [10] (Granger, 1969);
D) First-stage WI tests for vector $\beta_0 = 0$ in eq. (9.1): AR, LM, LR (Yogo, 2004);
E) First-stage relevance tests: minimum eigenvalues of the Concentration Parameter matrix and Cragg-Donald test statistic (Stock and Wright, 2000; Stock et al., 2002);
F) First-stage joint instrument exogeneity and relevance LR-type test (Kim and Lee, 2009); standard and asymptotic AR tests for overidentifying restrictions (Anatolyev and Gospodinov, 2010);
G) GMM standard *J* statistic (Hansen, 1982) and asymptotic *J* statistic (Imbens et al., 2003), both used to test the validity of the overidentifying restrictions;
H) GMM standard and asymptotic AR statistics tests for vector β_0 evaluated at the parameter estimate and validity of the overidentifying restrictions (Andrews and Stock, 2007);
I) GMM key statistics of the estimated residuals;
J) GMM coefficient vector and t statistics or WI-CI (e.g. Moreira, 2003; Cruz and Moreira, 2005; Kleibergen and Mavroeidis, 2009);
K) GMM Kleibergen's tests for vector $\beta_0 = 0$, namely, the standard Wald test and RK, S, KLM, J KLM and MQLR statistics described in Sect. 3.1.

The first category of pretesting (A and B) to be implemented is represented by the determination of the true number of regressors and of instruments in presence of a large dataset. It is a powerful alternative to traditional PCA methods utilized to compute the number of factors, (e.g. Anderson, 1984), which are shown by Bai and Ng (2002, 2008) not to produce consistent results as $T, K \to \infty$.

This method is based on PFA and PCA, and is unanimously refered to as "factor modeling" or Factor IV (FIV) estimation. It can easily cope with many regressors without running into scarce degrees of freedom problems or in collinearity, and it is utilized to reduce in a first place the number of regressors, chosen among the widest possible available set, including variables that may be either justified or unjustified on theoretical grounds.

In its simplest form, FIV builds upon the common-component static factor model developed by Chamberlain and Rothschild (1983), where the true number *r* of factors is unknown ex ante and can be endogenously determined by formal statistical procedures characterized by information criteria, reported in Appendix 2, that place penalties on large datasets (Bai and Ng, 2002, 2007). The few and most relevant factors so obtained, in terms of computed shares, contain most of the model's information and may be supplemented – if necessary – by additional regressors or instruments to form the entire available dataset.

The second category (C to F) includes first-stage testing of eqs. (9.1) and (9.2). They are well renowned in the current practitioner's literature except for the last ones, which are of recent date. The first of these is denoted Q_{IV} by its authors (Kim and Lee, 2009), while the second is an AR test adjusted for the number of instruments (Anatolyev and Gospodinov, 2010). Q_{IV} is a joint test for the IV instrument relevance and exogeneity with respect to structural errors, and is derived from two competing model specifications: one with exogenous and the other with irrelevant instruments. The Q_{IV} test is based on the LR of these two models; hence the joint null hypothesis is $H_0 : \beta = 0,\ \Pi = 0$ from eq. (9.1) and (9.2) respectively. In other words the null is represented by both exogeneity and irrelevance, and has a peculiar quasi χ^2 distribution whose critical values are tabulated by the authors via MC simulation draws, although only for $K \leq 3$ regressors. If the Q_{IV} test statistic obtained from sample estimation rejects the null the instruments are deemed of good quality, and thus relevant, but not necessarily exactly exogenous.

The standard AR test statistic for overidentifying restrictions may be supplemented by a statistic bearing an asymptotic corrected size that prevents too frequent overrejections of the null hypothesis, determined by (moderately) many instruments. Anatolyev and Gospodinov (2010) found a similar occurrence with the standard *J* statistic, characterized by underrejection, and proposed an equivalent asymptotic test statistic. Both corrections build on foregoing work, where some authors have devised asymptotic corrected counterparts of the *J* and AR tests: the $J_{ASY} = \dfrac{J-L}{\sqrt{2L}}$ and the $AR_{ASY} = \sqrt{L}\left(\dfrac{AR}{L} - 1\right)$ tests, respectively distributed as $N(0,1)$ and $N(0,2)$ statistics (Imbens et al., 2003; Andrews and Stock, 2007).

Standard GMM-estimated residual statistics (category I) include the following: Standard Error (SE), Durbin-Watson statistic for first-order autocorrelation and ARCH test for heteroskedasticity (Engle, 1982), as well as the first-order autocorrelation coefficient that has been previously used as a selecting device for the appropriate data filtering (Sect. 3.1) and that can here perform a similar task on grounds of consistency.

3.3. The Dynamic GMM and the Construction of Dynamic Principal Components

Eq. (9.1) can be extended to produce the following dynamic estimating equation:

10) $$\Delta y_t = \mathrm{X}_t B(\lambda)' + e_t(\lambda)$$

where $B(\lambda) = \left[\mu_1, \mu_2, \tau_1, \tau_2, \xi_1, ..., \xi_{K_1}\right]$ and ξ_k, $k = 1,..., K_2$, are the coefficients of $\tilde{X}_t$, $\forall \lambda \in \Lambda$. Finally, $e_t(\lambda) = I.I.D.(0, \sigma_e^2)$ and $\mathrm{E}\left(\mathrm{X}_t(\lambda)' e_t(\lambda)\right) = 0$.

Eq. (10), just as eq. (2), enables constructing a time series of length $1 + (1 - \lambda_0)T$ of the coefficient vector $B(\lambda)$ and of the ensuing two *t* statistics $\hat{t}_\mu(\lambda)_t$ and $\hat{t}_\tau(\lambda)_t$ [11]. GMM estimation of $B(\lambda)$ requires the introduction of an *L*-sized Z_t instrument set $(L \geq K)$. In many cases, Z_t is represented by lag transformations of the set $\tilde{X}_t$ such that $Z_t = \left[1, \tilde{X}_{t-m}\right]$ for $m = 1,...M$ lags. In other cases, and specifically when expectations are assumed to be the driving cause of the behaviour of the endogenous variable (e.g. the Taylor Rule, Clarida et al., 2000), the vector $\tilde{X}_t$ is augmented with its own leads and K_2 may be large. In such case, also the vector of instruments Z_t must be lengthened with the risk of producing, however, the many WI curse (Stock et al., 2002) for $L \longrightarrow \infty$, even if $T \longrightarrow \infty$.

The *L*-sized vector of sample moments, each being a random process of length $(1-\lambda_0)T$, is

$$g_t(\hat{\beta},\lambda) = Z_t \otimes \hat{e}_t(\lambda)$$

where the coefficient vector $\hat{\beta}$ and the first-stage residuals $\hat{e}_t$ stem from a (possibly) consistent TSLS estimation of eq. (10). The sample means of the above are

$$\overline{g}\left(\hat{\beta},\lambda\right) = \left[(1-\lambda_0)T\right]^{-1} \sum_{t=\lambda_0 T}^{(1-\lambda_0)T} g_t\left(\hat{\beta},\lambda\right)$$

with the orthogonality property that $E\left[\overline{g}\left(\hat{\beta},\lambda\right)\right] \equiv 0$, a necessary condition for instrument exogeneity. Let also the ensuing long-run p.d. weight matrix be

11) $$W(\hat{\beta},\lambda):(L \times L) = \left[(1-\lambda_0)T^{-1}\right] \sum_{t=\lambda_0 T}^{(1-\lambda_0)T} g_t(\hat{\beta},\lambda) g_t(\hat{\beta},\lambda)'$$

such that $\hat{\beta}_{GMM}(\lambda) = \arg\min_{\beta \in \mathrm{B}} \left(\overline{g}(\hat{\beta},\lambda) W(\hat{\beta},\lambda)^{-1} \overline{g}(\hat{\beta},\lambda)\right)$.

Computation of the partial first derivatives of the sample moments yields the $KL \times L$ Jacobian matrix

12) $$G_t(\lambda) = \left[(1-\lambda_0)T^{-1}\right] \sum_{t=\lambda_0 T}^{(1-\lambda_0)T} z_t x_t'$$

where z_t, x_t respectively are the *L*.th and the *K*.th element of vectors Z_t and X_t. For relevance, we expect the Jacobian to be of full rank and no zero minimum Singular Value (SV). Finally the efficient GMM estimator, by letting $Z'y = \sum_{t=\lambda_0 T}^{(1-\lambda_0)T} z_t \Delta y_t$, is

13) $$\hat{\beta}_{GMM}(\lambda) = \left[G_t'(\lambda) W(\hat{\beta},\lambda)^{-1} G_t(\lambda)\right]^{-1} G_t'(\lambda) W(\hat{\beta},\lambda)^{-1} Z' y_t$$

where, specifically

14) $$\hat{\beta}_{GMM}(\lambda) = \left[\hat{\mu}_1, \hat{\mu}_2, \hat{\tau}_1, \hat{\tau}_2, \hat{\xi}_1, \ldots, \hat{\xi}_{K_1}\right]$$

whose asymptotic normality property is

$$T^{1/2}\left[\hat{\beta}_{GMM}(\lambda) - \beta^*\right] \xrightarrow{d} \mathrm{N}\left(0, S(\hat{\beta},\lambda)\right)$$

where

15) $$S(\hat{\beta},\lambda) = \left[G_{(1-\lambda_0)T}'(\lambda) W(\hat{\beta},\lambda)^{-1} G_{(1-\lambda_0)T}(\lambda)\right]^{-1}$$

is the "sandwich" matrix.

In the presence of autocorrelation and/or heteroskedasticity of $e_t(\lambda)$, that is, of persistence in the error term, the weight matrix of eq. (11) must be augmented in the form of the long-run covariance matrix

16) $$W(\hat{\beta},\lambda)=\sum_{s=-(1-\lambda_0)T+1}^{(1-\lambda_0)T-1} k\left(\frac{s}{b}\right)\Gamma(s,\lambda),$$

where *k* is a preselect kernel function (e.g. Bartlett, Parzen, etc.), *b* is the bandwidth and

17) $$\Gamma(s,\lambda)=\left[(1-\lambda_0)T^{-1}\right]\sum_{t=\lambda_0 T}^{(1-\lambda_0)T} g_{t+s}(\hat{\beta},\lambda)g_t(\hat{\beta},\lambda)'$$

is the *s*.th sample autocovariance of $g_t(\hat{\beta},\lambda)$; $s=0,\pm1,...$ (Newey and West, 1987; Smith, 2005). Consistency of eq. (17) requires that $(1-\lambda_0)T>b>0$ and that $b\to\infty$, $b/(1-\lambda_0)T\to0$ as $T\to\infty$ i.e. that downweighting of $\Gamma(s,\lambda)$ operated by the smoother in eq. (16) be such as to produce a covariance matrix biased toward zero (Kiefer and Vogelsang, 2002). In common practice, the optimal value of *b* is (automatically) chosen to minimize the asymptotic mean square error of eq. (16).

Let $\mathrm{X}_t:(T\times K)$ as defined in Sect. 3.1. By virtue of the Spectral Decomposition Theorem, define the symmetric asymptotic covariance matrix $\mathrm{X}_t'\mathrm{X}_t/\mathrm{T}=\mathrm{ERE}$, where, for $X_t=\left[1,t,DU_t(\lambda),DT_t(\lambda)\right]$, $\mathrm{X}_t=\left[X_t\,\vdots\,\tilde{X}_t\right]$ and $K=K_1+K_2$, $\mathrm{T}:(K\times K)$ is a rate-of-convergence matrix with an upper left matrix $(K_1\times K_1)$ constituted by four 2×2 submatrices each containing $\begin{bmatrix} T & T^2 \\ T^2 & T^3 \end{bmatrix}$, and 2 row and 2 column vectors $(K_2\times1)$ of trailing $T^{3/2}$ placed in correspondence of the time-related deterministics, that is, at $K_1=2,4$. All other entries of matrix T are given by ones.

In addition, R is the $K\times K$ diagonal matrix of the eigenvalues r_i, $(i=1,...,K)$ in descending order, and E the same sized matrix of eigenvectors with column elements E_j, $(j=1,...,K)$. We have $E(\mathrm{E'E}=I_K)$, where I_K is the $K\times K$ identity matrix that ensures orthogonality of the principal component scores, which correspond to those in PFA (Appendix 2).

For each E_j, define the scalar $\eta_j=\arg\max(\mathrm{E}_j)$, $(j\neq i)$ such that the static PCA shares, corresponding to the eigenvalues in descending order, are described as

18) $$s_i=(r_i\,|\,\eta_j)\Big/\sum_{i=1}^{K}r_i$$

where $(r_i\,|\,\eta_j)$ denotes the association between the *i*.th eigenvalue and η_j.

After defining α_j the *j*th regressor's marginal significance of the coefficient, the time series of length $1+(1-\lambda_0)T$ of the *j*th regressor's dynamic and significance-weighted share measured over the trimmed interval $t\in\{\lambda_0T,(1-\lambda_0)T\}$ may be expressed as

19) $$s_i(\lambda)=\left[(1-\alpha_j)(r_i\,|\,\eta_j)\Big/\sum_{i=1}^{K}r_i\right](\lambda);\ \forall\lambda\in\Lambda,$$

where $(1-\alpha_j)$ is the appropriate weight assigned to the *i*th share. Eq. (19) provides the dynamic PCA time series of the shares to be exploited in the following Sections.

Apart from the dynamics involved, eq. (19) is preferable to eq. (18) because it weighs each component share by the statistical significance appended to its coefficient. Traditional PCA (e.g. Anderson, 1984), by ignoring this evidence and by sticking to nominal shares, may overstate in quite a few instances the components whose role is empirically found to be virtually close to zero. In alternative, the $1-\alpha_j$ weight may be substituted for by the *t* statistic of the *i*th coefficient. The advantage is represented by a 'double weighting' which includes also the absolute magnitude of the coefficient involved, and not only its standard error.

4. The Climate-related Dataset and the Empirical Estimations of Global Warming

In this Section all the climate-related data are exhibited together with an index of GW and then subjected, after appropriate filtering, to empirical estimation by dynamic GMM. Before proceeding, it is worth reminding the gaseous composition of Earth's atmosphere: Nitrogen (N_2, 78%), Oxygen (O_2, 20%) and a few more, among which Carbon Dioxide (CO_2), Methane (CH_4), Nitrous Oxide (N_2O) and Nitrogen Dioxide (NO_2). For ease of reading, the reported Mendeleyev symbols are respectively simplified as follows: N2, O2, CO2, CH4, N2O and NO2. Apart from water vapor, Chloro-Fluoro-Carbons (CFCs) and composite anthropogenic and natural aerosols, CO2, CH4 and NO2 purportedly reduce or trap the loss of Earth's heat into space and cause – under certain conditions – the renowned "Greenhouse effect" and the consequential GW.

However, while GW is a minor part of the Earth's long climatic history, other forcings at present and in the past times are held responsible of climate changes, although in many cases the data availability and affordability pose a restraint to large-scaled modeling addressed at event simulation, prediction or causative analysis. Precisely to this very end, the purpose of this Section is to introduce the available dataset and to perform such analysis for the sake of the advancement of knowledge.

4.1. Global Warming and Climate Forcings during the Period 1850-2006

Planet Earth has passed through many waxing and waning climate episodes during the entirety of its life. For instance, the Mid-Cretaceous (120-90 million years ago) and the Palaeocene Eocene Thermal Maximum (PETM, 55 million years ago) have experienced temperatures distinctly warmer than today, with animals and plants living at much higher latitudes and with higher carbon dioxide (CO2V) levels, roughly two to four times than the present-day ones.

Abrupt climate changes have occurred also during the more recent Phanerozoic eon (Shaviv and Veizer, 2003), like the last glacial period (Alley, 2000), the Medieval Warm Period, centered around 1000 A.D., apparently the warmest period so far in the Christian era (Esper and Frank, 2009), and the Maunder Minimum in Europe during the years 1645-1715 A.D. Fig. 1a provides an account of the climatic oscillations that have occurred in the last twelve centuries or so, which are significantly proxied by the time series of the North Atlantic Ocean Mode (Trouet et al., 2009). Clearly, the Medieval Warm Period and the current GW represent the peaks, as found by other researchers too that use different proxies (Bürger, 2007).

Many of the climate changes have affected human activities, like the disappearance of the Neanderthal man and countless population migrations, e.g. the Siberian exodus toward the Americas, the Dravidian occupation of Ceylon, and the short-lived experience of the Vikings in Greenland. In quite a few cases, climate changes are even held responsible, although not entirely, for the collapse of some civilizations like the Akkadians and the Mayans, struck by severe droughts respectively in the 22nd century B.C. and 800-900 A.D. (Gill, 2000; Cullen et al., 2000). Many more human-driven episodes have directly affected climatic conditions and local environments: for instance the desertification of Northern Africa partly commenced since the late Roman Empire and that of Australia, caused by extensive slash-and-burn practices of the aboriginals.

While the above cited may be casual episodes of the often perverse relationship between humans and nature, the by now secular GW phenomenon, more recently dubbed "climate change" by the majority of its mentors, is undoubtedly cause of concern. In fact, the last hundred years or so have experienced a renewed climate change after the Maunder Minimum by exhibiting a rise in the mean global surface temperature by about 0.6 ± 0.2°C since the late 19th century, and by about 0.35 ±0.05° C over the last 40 years (Chenet et al., 2005). This phenomenon, while not unique in Earth's history (Baliunas and Soon, 2003) as shown in Fig. 1a, has spurred intense debate on the analysis of its causes and is by now a worldwide major issue which involves popular media, scientists, corporations, governments and political organizations.

In fact, while the rise in temperatures is of undisputed evidence, yet at a slower pace in the last decade, the search for a main culprit is still in progress and well alive, and is being characterized by two opposing fronts regarding its causes: the advocates and the skeptics of its anthropogenic origin. Either sides hold on to their own positions since a decade or more and recent scuffles, such as the "Climategate" affair and the "hockey-stick" controversy demonstrate the vitality of the confrontation.

Advocates of the human-induced greenhouse effects, purportedly caused by CO2 emissions and industrial aerosols, include several scientists (e.g. Hansen et al., 2007), the UN-mandated Nobel-prized Intergovernmental Panel on Climate Change (IPCC) and large sections of governments and politicians[12].

Skeptics, on the other hand, form a scientifically-based consensus that supports and proves the prevalence of long-run evolving natural causes, defined as "global forcings", like solar activity (Abdussamatov, 2004), Cosmic Ray Flux (CRF) (Shaviv and Veizer, 2003; Svensmark, 1998; Bard and Frank, 2006, Usoskin et al., 2003), volcanic aerosols (Mann et al., 2005) and ocean currents (Gray et al., 1997). This consensus builds on reliable paleoclimatological dataset reconstructions (e.g. Crowley, 2000; Lean, 2000, 2004; Usoskin et al, 2003, 2004a, 2004b; Mann et al., 2005; Krivova et al., 2007), most of which are downloadable from the National Oceanic and Atmospheric Administration (NOAA) website.

The consensus share going to either group is not undisputed: according to a recent research (Doran and Zimmerman, 2009) the large-public opinion of Americans goes fifty/fifty, while more than 75% of peer-reviewed academic research papers backs the view that Earth's climate is affected by human activities. Other more recent sources of different origin express only little consensus on the anthropogenic causes of GW, and this has certainly dominated the choices made at the last IPCC Conference held in Copenhagen, December 2009.

One thing, however, stands clear to almost anybody: the analysis of the interaction of the variables implied in the secular GW process is very complex, as it requires countless and valuable in-depth experimenting stemming from different scientific fields, such as astrophysics, climatology, biology and chemistry. Statistics and econometrics may contribute to the current state of knowledge by supplying interesting insights into causality occurring in a casual environment. Not much work has been produced hitherto in this field, except for few though valuable contributions (e.g. Lanne and Liski, 2004; Kaufmann et al., 2006). Certainly more will come in the future.

GW is identifiable with data sets on land and sea temperature recordings collected by different agencies for select periods, areas, altitudes, hemispheres, etc. The Best Estimated Anomaly (BEA) of the updated HADCRUT3 dataset (Brohan et al., 2006), available for the period 1850-2006 on an annual basis, was selected due both to its space and time breadth. Therefore, the BEA index represents the endogenous variable used in eq. (10), whose GMM estimated parameter vector is given by eq. (14).

In line with BEA, which constitutes a time series of 157 observations and is used as synonym of GW and climate change[13], an ample dataset of climate forcings was retrieved from different sources worldwide available over the internet, and especially from the NOAA website. The list of forcings which play the role of regressors and instruments in GMM estimation is exhibited in the Data Description and Sources, and is made of the following two main categories:

anthropogenic and natural forcings. Their tally is 37, of which 14 of anthropogenic origin and the others of natural or mixed origin.

The anthropogenic forcings include average real GDP percapita of the total 12 Western Europe major countries and of its overseas offshoots (U.S.A., Canada, Australia and New Zealand), and their total population (Maddison, 2007)[14]. They are respectively labeled INCOME_E, INCOME_O, POP_E and POP_O. Anthropogenic forcings also include the components of trace or greenhouse gases (GHG) that characterize air pollution. They are given by four measures of emissions: carbon dioxide (CO2) expressed in terms of global volume, which includes emissions from fossil-fuel burning, cement manufacture, and gas flaring (Marland et al., 2007), and final emissions of CO2, methane (CH4) and nitrous oxide (N2O), expressed in terms of Radiative Forcing (RF) measured in Watts per square meter (W/m2) (Robertson et al., 2001). Global sulphur emissions, expressed in thousands of metric tons, are also available (Stern, 2002). These forcings are respectively labeled as: CO2V, FCO2, FCH4, FN2O and GSULFEM. While the first and the last variable may be considered as a stock, the other three are a flow.

Needless to say, a part of the CO2-based emissions derive from the Global (oceans and land) Carbon Cycle, whose emissions and suspension in the atmosphere absorb radiation emitted from the Earth, trapping heat and contributing to GW, but at the same time shield the Earth from the Sun's radiation, volcanic and geothermal activity, large forests, and man-made fermentation processes (e.g. beer and whiskey). Similarly, a part of CH4-based emissions derive from natural decay present in wetlands (e.g. swamps and marshes), urban landfills and waste treatment, livestock, volcanic activity, etc. Mostly man-made are instead N2O-based emissions deriving from internal combustion of engines, rocket motors, aerosol spray propellants, as well as analgesic & anesthetic products.

The category of natural forcings includes measures related to solar, volcanic and combined activities, as well as to cosmic rays and oceanic modes. As far as solar activity is concerned, there are 9 indicators: the average yearly number of monthly sunspot series (NGDC, 2007), a measure of total solar irradiance received at the outer surface of Earth's atmosphere in terms of RF (Krivova et al., 2007), tropical solar RF (Mann et al., 2005), composite solar RF, composite volcanic RF, and a total of four measures of Beryllium 10 (BE10) and Radiocarbon 14 (C14) that proxy solar RF (Crowley, 2000). In sequence, these forcings are labeled as: SUNSPOTS, SOL, SIR, TSI, COMPSOL, C14RLS, C14BLS, BE10BS and BE10LS.

Volcanic activity is represented by tropical and composite volcanic RF (Mann et al., 2005), and by a binary index that dates the major tropical eruptions (Ammann and Naveau, 2003), while oceanic modes are represented by Pacific Decadal Oscillations (Shen et al., 2006) and the North Atlantic Ocean Mode (Trouet et al., 2009). They are sequentially labeled as: VOL, COMPVOL, VOLER, PDO and NAOM. In addition, cosmic ray activity is proxied by the CRI flux (Usoskin et al., 2003; Alanko-Huotari et al., 2006), while the combined effects of volcanic and solar activities are proxied by the RF of the VOLSOL indicator (Mann et al., 2005). Natural and anthropogenic combined effects in the form of tropospheric aerosols are represented by sulphur and fossil-fuel black carbon emissions in volume and in RF (Crowley, 2000), respectively labeled as AEROSOL and AERF.

Finally, a climate-related valuable database (Stern, 2002, 2004) is added. It includes several indicators of human and natural origin, mostly adjusted variants of above-listed forcings. These are the world total sulphur emissions expressed in megatons, labeled as GSULFEM, and the radiative forcings from carbon dioxide, methane, nitrous oxide, two measures of chlorofluorocarbons responsible for ozone depletion, anthropogenic sulphur emissions, and two measures of volcanic and solar activities, respectively. All these variables are labelled as: CO2, CH4, N2O, CFC11, CFC12, SOX, VOLGL and SOLS.

When unavailable for the more recent years, the data series of the 37 forcings are all updated to the year 2006 by means of forecasting via the autoregressive method, with lags selected via minimum BIC. Table 3 reports some descriptive raw statistics of BEA and of all the given forcings. Of interest are the large differences between the minima and the maxima of NAOM, PDO, some anthropogenic forcings and volcanic activity, expressed in terms of their volatility coefficients. Also, the CO2-based and some anthropogenic forcings appear to be nonstationary as revealed by the *p*-values of the ADF *t*-test statistics. Oddly enough, BEA reveals stationarity, a feature confirmed also by other findings (fn. 15).

Thereafter, all level forcings – logged when applicable[15] – are made to undergo appropriate HP filtering (excluding VOLER which is a dummy) and their cyclical components are extracted for the purposes of empirical estimation. The smoothing parameter chosen for the entire dataset is 6.25 as suggested by Ravn and Uhlig (2001). The rationale for this choice is based on the ARCH and autocorrelation coefficient results of the pretesting conducted on the structural equation (9.1) along the lines suggested in Sect. 3.1.

Therefore, alternative specifications of the equation include different sizes of the vector of forcings (K), ranging from a minimum of two to a maximum of eight true factors selected from the 37 forcings available (Bai and Ng, 2002, 2007, 2008), and of the instruments, whose size is chosen in all cases to be L=2K. For each specification, larger HP smoothing parameters (100 and 400), first differencing, and centering and scaling have also been applied to all variables. The latter alternatives, however, produced unsatisfactory or less satisfactory results and were therefore dismissed as candidates for data transformation[16].

Fig. 1b illustrates the levels and the HP-filtered values of the logs of BEA and of all forcings. From the left panel, GW can be shown to exhibit a trending behavior since 1850[17], which is ostensibly stationary when appropriately filtered. The human forcings exhibit a trend, but methane (FCH4) seems to taper off in the last decade. On the other hand, the natural forcings are mostly cyclical, with SUNSPOTS exhibiting a known regularity of around 11 years. While retaining their labels, all of the variables used in calculations and estimations that will follow are henceforth understood, unless otherwise defined, to be represented by their HP-filtered magnitudes (see fn. 12).

4.2. Expected Effects of Forcings over Global Warming

The 37 listed forcings by means of ongoing research are expected to bear specific effects over the World temperature changes represented by BEA. Of the human forcings, economic activity and the size of population (INCOME and POPULATION) are expected to raise BEA via GHG emissions, extensive deforestation and generalized use of inefficient technologies. The United States and China nowadays appear by some estimates to be the main responsible for CO2V volume emissions, and especially the second is poised to double its GHG emissions within a decade or so.

Solar activity manifests itself in different forms that may significantly affect climate variability. Sunspot numbers (SUNSPOTS), total solar irradiance (TSI) and solar cosmic rays (CRI) are highly correlated and constitute the ensemble of "solar forcings". Their long-run reconstructions stem from direct measurements, like the sunspot numbers supplied since Galileo, or from solar proxy variables like the accumulated layers of BE10 in ice cores and C14 in tree rings. Whether directly or through cloud formation or by changes in the Earth's albedo, solar forcings are in many cases shown to sizably affect the Earth's climate (Usoskin et al., 2003, 2006; Solanki et al., 2004; Shaviv and Veizer, 2003; Svensmark, 1998). In particular, increased sunspot activity – according to some theories – causes a cooling of the Sun's surface by trapping its energy output. This was evidenced by telescope measurements made from 1976 to 1980, which showed that the Sun's surface had cooled by about 6° C as the number and size of sunspots increased. However, the matter is debated, since according to other theories the correlation between climate changes and sunspot numbers is positive (Baliunas and Soon, 2003) although mediated through measured TSI.

Some authors (Solanki et al., 2004) have recognized that the level of solar activity during the past 70 years is exceptional, and that the previous period of equally high and prolonged activity had occurred more than 8,000 years ago. They found that during the past 11,000 years the Sun has produced, on average, only 10% of the time a similarly high level of magnetic activity and that almost all of the earlier high-activity periods have been shorter than the present episode. In spite of the rarity of the current episode of high average sunspot numbers, however, the authors point out that solar variability is unlikely to have been the dominant cause of the recent climate changes, and especially of those occurred during the past thirty years. A similar conclusion is reached by other authors (Rind et al., 2008) who make use of complex modeling supplied by the Goddard Institute for Space Studies (GISS).

TSI is expected to raise the Earth's temperatures via increased luminosity, although there is no general agreement on its size and significance, since its variability (only 0.1%-0.2% over the 11-year cycle) is so low as to deserve the nickname of 'solar constant' (Fouka et al., 2006). TSI is likely to operate in conjunction with the CRF by negatively affecting climate via low-altitude cloud cover and increased rainfalls (Svensmark, 1998; Svensmark and Frijs-Christensen, 2007; Shaviv, 2005). Finally, the effects of PDO and similar oceanic currents on the overall climate are uncertain insofar as this variable appears to be driven, partly, by solar forcing fluctuations (Shen et al., 2006) and partly by the El Niño-Southern Oscillation (ENSO) while its cycling magnitude has not yet been ascertained (Gray et al., 1997; McDonald and Case, 2005).

Volcanic activity is also poised to affect climate, especially in the Northern Hemisphere (Shindell et al., 2004). The release of aerosols rich of sulphates and CO2V reflects sunlight away from the surface of the Earth causing a climate cooling due to dust veils (*tephra*) suspended in the atmosphere. At the same time, however, aerosols absorb solar and infrared radiation leading to warming of the surrounding air masses. This applies in particular to large volcanic eruptions whose effects may last for years, as in occasion of the eruptions of Krakatoa in 1883, El Chichón in 1982 and Pinatubo in 1991. The net effect on overall climate is therefore still matter of dispute (Shindell et al., 2004; Mann et al., 2005; Chenet et al., 2005).

The IPCC defends since at least a decade the anthropogenic hypothesis by stating in its Third Assessment Report (AR3 2001) that: "Forcing due to changes in the Sun's output over the past century has been considerably smaller than anthropogenic forcing…Its level of scientific understanding [is] very low, whereas GHGs forcing continues to enjoy the highest confidence level….[and] the temporal evolution indicates that the net natural forcing has been negative over the past two and possibly even the past four decades….[It is therefore] unlikely that natural forcing can explain the warming in the latter half of this century".

In its Fourth Assessment Report (AR4, 2007) the IPCC, while maintaining that: "There is very high confidence that the net effect of human activities since 1750 has been one of warming", issues severe warnings about melting glaciers and Polar ice sheets, increased hurricane intensity due to substantial changes in wind patterns, average sea level rise, worsening droughts and heavier precipitations and, finally, a growing gap between human-driven and solar RFs. Warming would thus be attributed to solar forcing by a 10% share with the remaining 90% attributable to human forcing in terms of GHG emissions, supposedly capable of absorbing infrared energy within the troposphere[18].

4.3. Static GMM Model Selection and Preliminary Empirical Results

As advanced in the Introduction, testing for breaks in the time series of GW and its causes is equivalent to testing for the null hypothesis of its anthropogenic nature. Natural causes during the period 1850-2006, in fact, do not exhibit any known substantial break worldwide. Moreover, as will be found shortly, anthropogenic forcings do not even enter significantly the determination of GW.

The detection of single and multiple breaks obtained by means of popular methods for SBA, e.g. the Zivot-Andrews (1992) and of the Bai-Perron (2003) procedures, produces conflicting results which are very sensitive to both the lags of the endogenous variable (BEA) and of the forcings included[19]. This is an additional reason for proceeding, after performing the optimal static GMM model selection, along the lines of the proposed dynamic method so as to analyze the time series of breaks, coefficient and shares of the forcings that determine GW.

Table 4 supplies the pretest battery of results introduced in Sect. 3.2 that is utilized for the optimal static GMM model selection, i.e., for the 'best' specification suitable for estimating the structural equation (9.1) and for proceeding in the next Section to the Dynamic GMM estimation. All the variables, including the endogenous BEA but excluding VOLER, are understood to have been HP-filtered by a smoothing factor of 6.25 (Sect. 4.1). The procedure adopted for such selection utilizes several specifications of eq. (9.1), with the number of true factors ranging from two to eight, found among all the 37 forcings. A linear trend and a constant are included in the estimation but are not exhibited, and the instruments are the 1-2 lags of the true forcings, including a linear trend and a constant.

The true factors retain the original labels of the associated HP-filtered variables and their list is exhibited in the first pane of Table 4.What immediately shows up even by cursory inspection is the inclusion of natural forcings only, and specifically those related to oceanic current cycles, as well as to solar and volcanic activity. No anthropogenic or mixed forcing appears in the sequence. The procedure here adopted for model selection is the same as the one previously adopted for data filtering (Sect. 4.1), but in addition the model selected should be characterized by the following:
i) the endogeneity of some or all forcings should be significantly detected, or else GMM estimation collapses to OLS;
ii) the null hypothesis $H_0: \beta = 0$ under possible WI in both the first-stage TSLS and even more so in the two-step GMM estimation should be significantly rejected;
iii) the relevance and exogeneity of the selected instruments should be proven, elsewise all standard tests fail to deliver the appropriate inferential information;
iv) the true factors selected (Bai and Ng, 2002, 2007, 2008) should exhibit in most cases significant *t* statistics.

The results reported in Table 4 suggest in panel C that endogeneity of some forcings is present, namely, SUNSPOTS and VOLER when assuming causality is running from the residuals to the forcings and PDO, COMPVOL and VOLSOL when assuming the opposite direction of causality. At least intuitively, the latter appears to better represent the phenomenon of endogeneity and, strictly speaking, the last three variables should be instrumented.

While the minimum eigenvalues of the Concentration Parameter matrix and the Cragg-Donald test statistics point to first-stage relevance of the instruments for all specifications (panel E), the first three specifications do not pass, below a *p*-value of 10% , the null hypothesis $H_0: \beta = 0$ for the first-stage (panel D) and for the GMM AR test statistics (panel H), nor the tests of joint exogeneity and relevance (panel F), nor even the standard and asymptotic *J* test statistics for exogeneity (panel G). This outcome is revealing of the fact that small-sized vectors $(K \leq 3)$ of true factors are inappropriate for estimation in the present context, as they definitely entail weak and/or endogenous instruments. Larger-sized specifications $(4 \leq K \leq 8)$ involve instead highly significant test statistics, an evidence that is confirmed for GMM by Kleibergen's test battery (panel K) which involves rejection of $H_0: \beta = 0$ for specifications where $K > 3$, although somewhat below the *p*-value of 10% on average.

On the other hand, the poor result of the *J* test statistic for instrument exogeneity with $K = 8$ (line 7, panel G) indicates the existence of too many instruments, and the *p*-value of its asymptotic counterpart does not fare better than smaller-sized specifications. While from panel I heteroskedasticity as measured by the ARCH(1) statistics seems unavoidable for all specifications, the Durbin-Watson statistic points to some level of error negative autocorrelation with $K = 5$ and $K = 8$, although not much more significantly than the other specifications. The *JKLM* statistic for the above null and for instrument exogeneity produces a comparatively interesting result with $K = 7$ insofar as the other specifications have been ruled out for the reasons above mentioned.

In summary, after assigning due weight to each selection method, the GMM model specification with $K = 7$ is selected. Panel J of Table 4 exhibits the coefficients and related *t*-

statistics output, which is reproduced for ease of reading in Table 5. The weighted shares therein shown are constructed according to eq. (19), the weights being the *t* statistics of the coefficients. The most striking results are the coefficient signs: negative for PDO and moderate volcanic activity, and positive for SUNSPOTS and intense volcanic activity. Hence, world average temperature trends are the result of mutually outweighing natural forces related to both Earth and Sun, with almost equal coefficient sign-based weighted shares. In practice, negative and positive effects over climate changes participate each by 50%.

4.4. Time Series of Breaks, Coefficients and Weighted Shares of the Selected GMM Model

The selected specification is then estimated according to eq. (10) and produces eq. (14). The trimming factor is different for each end: $\lambda_0 = 0.10$ and $1-\lambda_0 = 0.05$, so that after rounding the estimated period span is 1865-2000. Fig. 3 shows for this period the time series of the *t* statistics of the two structural breaks: the level break $t_T(\lambda, L)$ and the trend break $t_T(\lambda, T)$, namely, eqs. (8.1) and (8.2). They exhibit a jagged behavior around a zero mean, as expected from Sect. 2, and the minima and maxima of the former and of the latter are well beneath the critical values tabulated in Table 1, indicating that no significant break whatsoever has occurred during the period under scrutiny[20].

The variances of the *t* statistics of the constant, of the trend and of the respective breaks are: 0.6022, 0.3373, 1.7031, and 1.1105, while the corresponding estimated volatilities are: -1.0054, 0.6442, 3.7868, and 2.0968, while the mean variance and volatility of the other coefficient *t* statistics are close to zero. These results confirm the theoretical findings of Sect. 2 where the variance of the break statistics is proven to exceed unity even if they stem from unit-variance DGPs.

The coefficients of the forcings are essentially constant overtime and need not even be graphically illustrated. They retain the signs exhibited in Table 5, and the magnitudes of their own *t* statistics behave similarly. This constancy of the parameters implies stability of the causative effects of the forcings, as evidenced also by the above reported variances and volatilities. Then, SUNSPOTS and intense volcanic activity are constant warmers, each providing its role from above and beneath the troposphere, respectively. In particular, sunspot numbers are on average warmers because they raise total solar output and negatively affect mean cloudiness (Baliunas and Soon, 2003; Usoskin et al., 2003). In addition, large volcanic eruptions (e.g. Krakatoa and Pinatubo) are found to determine stratospheric heating due to ash spewing, lava emission and sulphur dioxide release which condensates in the atmosphere and traps the Earth's heat. Tropospheric cooling may ensue in the longer term causing "winter warming" via the tephra effect, thereby offsetting the initial rise in temperatures (Shindell et al., 2004).

Opposite to the warmers, PDO and moderate volcanic activity are constant temperature dimmers. The former, on average, is accompanied by negative sea surface temperatures related to the ENSO (Gray et al., 1997), while the latter cause limited gaseous emissions that do not determine greenhouse effects but prevent solar radiance to reach the Earth's surface.

Fig. 4 shows the HP-smoothed forcings weighted shares obtained by applying the dynamic PCA criterion introduced in Sect. 3.3[21]. While letting the explanatory role of coefficients unabated, the time-varying shares gauge the size of the contribution of each forcing in the variance of climate changes. Technically, the weighted shares are computed by using the asymptotic variance of the regressors X_t in the dynamic GMM, namely, the four deterministic variables and the given forcings as in eq. (19) where the weights are represented by the *t* statistics of the coefficients.

In Fig. 4 the weighted shares of the deterministics are not shown since they are very modest in magnitude, yet the share tally is somewhat smaller than unity. The largest weighted share found pertains to PDO, always above 40% and slightly increasing overtime, followed by SUNSPOTS, which averages 27% and is slightly decreasing, and by VOLER, which is close to 12% and rapidly increasing in the Nineties. The remaining shares tally around 10% and include VOL, VOLGL and VOLSOL. In sum, the contribution of volcanic activity is on average 27% and is slightly increasing overtime while, in spite of these evolutions, the weighted shares of dimmers and warmers are approximately equal in size as found in the above-reported statistics contained in Table 5.

5. Conclusions

The first and foremost finding of this paper is the following: human forcings of whatever nature are by no means responsible for the climate changes that have occurred on Planet Earth during the past 150 years. Moreover, along this period no significant break has ever occurred in the mean world temperatures that may be attributable to natural forcings either. While global warming is a phenomenon of undisputable evidence, although subject to a progressive tapering off, the current climatological science must acknowledge the negative impact of oceanic currents (PDO) and moderate volcanic activity, and the positive impact of sunspots and intense volcanic activity.

By consequence, mean world temperatures are the result of mutually outweighing natural forces related to both Earth and Sun. The role played in terms of weighted shares by each of these forces in climate trends determination is almost constant overtime, but exhibits a rise (fall) for PDO and most of volcanic activity (sunspots) since the last few decades or so. This performance, however, may not be utilized for predictive purposes, unless further research was produced.

These results demonstrate that the much-vaunted and daunting IPCC thesis of human forcing over climate change is seriously ungrounded by any empirical means and that its activity should be more seriously scrutinized and improved to avoid the dissemination of unjustified collective scares all around the Globe.

Data Description and Sources

1) BEA: Best Estimated Anomaly of global temperature records scaled to 14 degrees Celsius, HADCRUT3 dataset, Brohan et al., 2006.

2) SUNSPOTS: Yearly averages of monthly sunspot numbers, National Geophysical Data Center (NGDC), 2007.

3) SIR: Solar Irradiance Reconstruction, 11yrCYCLE, Lean, 2004.

4) TSI: Total Solar Irradiance RF reconstruction, Krivova et al., 2007.

5) CO2V: CO2 total emissions measured in million metric tons of carbon: Gas + Liquid and solid fuels + CO2 emissions from cement production + CO2 emissions from gas flaring, Marland et al., 2007.

6) CO2RF: Splice of CO2 Radiative Forcing post-1850 anthropogenic changes in equivalent greenhouse gas forcing, Crowley, 2000.

7) AERF: Tropospheric aerosols, Crowley, 2000.

8) INCOME_E, INCOME_O: Average of real GDP percapita of total 12 Western Europe, and its offshoots (GDDPC, 1990 International Geary-Khamis dollars), Maddison, 2007.

9) POP_E, POP_O: total population in Western Europe and its offshoots, Maddison, 2007.

10) Solar and volcanic forcings of the Tropical Pacific, Mann et al., 2005:

a) SOL: Solar RF, Mann et al;

b) VOL: Tropical Volcanic RF;

c) VOLSOL: Combined solar and volcanic natural RF, Model result estimates (Niño-3 index, anomalies in degrees C);

d) COMPSOL: Composite solar RF only, Model result estimates (Niño-3 index, anomalies in degrees C);

e) COMPVOL: Composite volcanic RF only, Model result estimates (Niño-3 index, anomalies in degrees C).

11) VOLER: Binary index of the major explosive volcanic eruptions, Ammann and Naveau, 2003.

12) PDO: Pacific Decadal Oscillation Reconstruction, Shen et al., 2006.

13) Trace Gases, Robertson et al., 2001:

a) FCO2: Carbon Dioxide, final globally averaged volumetric concentration in ppmv*;

b) FCH4: Methane, final globally averaged volumetric concentration in ppbv**;

c) FN2O: Nitrous Oxide, final globally averaged volumetric concentration in ppbv**.

14) GHG: Greenhouse gases, Crowley, 2000.

15) Solar variability reconstructions, Crowley, 2000:

a) C14RLS: C14 residuals /Lean splice;

b) C14BLS: C14 residuals Bard/Lean splice;

c) BE10BS: Be10/Bard splice, irradiance reconstruction of Bard et al., 2000;

d) BE10LS: Be10/Lean splice, irradiance reconstruction of Lean et al., 2000.

16) CRI: Cosmic Ray Intensity index, Polar Region Neutron Monitor count rate, Alanko-Huotari et al., 2006.

17) NAOM: North Atlantic Oscillation Mode (Multi-decadal Winter North Atlantic Oscillation Reconstruction), Trouet et al., 2009.

18) GSULFEM: Global sulfur emissions, millions of metric tons, Stern 2002, 2004 and updates from the author.

19) Radiative forcings, Stern, 2002, 2004:

a) CO2: Carbon dioxide;

b) CH4: Methane;

c) N2O: Nitrous oxide;

d) CFC11: Trichlorofluoromethane, and CFC12: Dichloro-difluoromethane;

e) SOX: Sulphur aerosols;

f) VOLGL: Volcanic aerosols;

g) SOLS: Solar irradiance.

---

* Parts per million in volume; ** Parts per billion in volume.

Appendix 1

Limit Distributions of the *t* Statistics of Level and Trend Breaks with Different Alternatives

The elements of eq. (5), for ε_t and σ from Δy_t^* given in the text (Sect. 2.1), are obtained as follows

$$T^{-1/2}\sum_{t=1}^{T}\varepsilon_t \xrightarrow{L} \sigma W(1), \qquad T^{-1/2}\sum_{t=\lambda_0 T}^{(1-\lambda_0)T}\varepsilon_t \xrightarrow{L} \sigma(1-\lambda)W(1)$$

$$T^{-3/2}\sum_{t=1}^{T}t\varepsilon_t \xrightarrow{L} \sigma W(1)-\sigma\int_0^1 W(r)dr, \quad T^{-3/2}\sum_{t=\lambda_0 T}^{(1-\lambda_0)T}t\varepsilon_t \xrightarrow{L} \sigma(1-\lambda)\left(W(1)-\int_0^1 W(r)dr\right)$$

while those of eq. (6) are derived from:

$$\sum_{t=1}^{T}1,\ \sum_{t=1}^{T}t,\ \sum_{t=1}^{T}t^2,\ \sum_{t=\lambda_0 T}^{(1-\lambda_0)T}(1-\lambda),\ \sum_{t=\lambda_0 T}^{(1-\lambda_0)T}t^2(1-\lambda) \text{ and } \sum_{t=\lambda_0 T}^{(1-\lambda_0)T}t(1-\lambda).$$

Finally, in eqs. (8.1) and (8.2)

$$\sigma^{-1}T^{-1/2}\sum_{t=1}^{T}\varepsilon_t \xrightarrow{L} W(1) \text{ and } \sigma^{-1}T^{-3/2}\sum_{t=1}^{T}y_{t-1} \xrightarrow{L} \int_0^1 W(r)dr.$$

These two Brownian functionals are distributed as follows:

$$W(1)\sim \mathrm{N}(0,1) \text{ and } \int_0^1 W(r)dr \sim N(0,1/3),$$

namely as a standard normal and as a doubly truncated normal with extrema close to 5% and to 95%, respectively. Hence, insofar as

$$E(W(1)) = E\left(\int_0^1 W(r)dr\right) = 0,$$

then

$$\underset{T\to\infty}{Lim}\left(\sigma^{-1}T^{-1/2}\sum_{t=1}^{T}\varepsilon_t\right)=0 \text{ and } \underset{T\to\infty}{Lim}\left(\sigma^{-1}T^{-3/2}\sum_{t=1}^{T}y_{t-1}\right)=0.$$

which implies that the two functionals tend to zero with different rates of convergence as *T* grows. Specifically, the Central Limit Theorem applies independent of λ.

Given the null and the alternative models represented by eqs. (1) and (2) in the text, here both replicated

A.1) $$\Delta y_t \equiv y_t - y_{t-1} = e_t$$

A.2) $$\Delta y_t = \mu_1(\lambda) + \mu_2(\lambda) DU_t(\lambda) + \tau_1(\lambda) t + \tau_2(\lambda) DT_t(\lambda) + \varepsilon_t(\lambda);\ \forall \lambda \in \Lambda,$$

the coefficients' limit distributions (Perron and Zhu, 2005) for $\varepsilon_t(\lambda) \sim I.I.D.(0,\sigma^2)$, are

$$T^{1/2}(\hat{\mu}_1 - \mu_1^*) = -\frac{2\sigma\left(\lambda W(1) - 3\int_0^1 W(r)dr\right)}{\lambda} \sim N(0, 4\sigma^2/\lambda),$$

$$T^{3/2}(\hat{\tau}_1 - \tau_1^*) = \frac{6\sigma\left(\lambda W(1) - 2\int_0^1 W(r)dr\right)}{\lambda^2} \sim N(0, 12\sigma^2/\lambda^3),$$

$$T^{1/2}(\hat{\mu}_2 - \mu_2^*) = -\frac{6\sigma\left(\lambda W(1) - \int_0^1 W(r)dr\right)}{\lambda(1-\lambda)} \sim N\left(0, 4\sigma^2/\lambda(1-\lambda)\right),$$

$$T^{3/2}(\hat{\tau}_2 - \tau_2^*) = -\frac{6\sigma\left(\lambda(3\lambda-1)W(1) - 2(2\lambda-1)\int_0^1 W(r)dr\right)}{\lambda^2(1-\lambda)^2} \sim N\left(0, 12\sigma^2\Phi\right)$$

where $\Phi = \dfrac{3\lambda^2 - 3\lambda + 1}{\lambda^3(1-\lambda)^3}$. These are indeed the diagonals of the square matrix in eq. (4.1).

The non-break *t* statistics of the constant (μ_1) and of the trend (τ_1) of eq. (A.2), respectively denoted as $t_T^*(\lambda, L)$ and $t_T^*(\lambda, T)$, are

A.2.1) $$t_T^*(\lambda, L) = \frac{3\int_0^1 W(r)dr - \lambda W(1)}{\lambda^{1/2}}$$

A.2.2) $$t_T^*(\lambda, T) = 3^{1/2}\frac{\lambda W(1) - 2\int_0^1 W(r)dr}{\lambda^{1/2}}.$$

The differences between the break and the non-break *t* statistics respectively are: $t_T(\lambda, L) - t_T^*(\lambda, L) \to \infty$, and $t_T(\lambda, T) - t_T^*(\lambda, T) <> 0$. The first tends to infinity for $\lambda \to 1$, while the second is negative for low values of λ and otherwise positive. In other words, the *t* statistic of the constant is always smaller than that of its break, and the *t* statistic of the trend is larger (smaller) than that of its break if λ is small (large).

The nonstandard distribution of the two non-breaks and of the two break statistics is obtained by dividing the above-shown coefficients' limit distributions by $\left(\Omega_T(\lambda)\right)^{1/2}$ and correcting for specific frequency windows. In particular, for the last two we have:

$$t_T(\lambda, L) \sim N\left(0, \frac{2\sigma^2\lambda^*}{\lambda^{1/2}(1-\lambda)^{1/2}}\right);\ \lambda^* = 1/2.5w^*,$$

where λ^* is a modified triangular window w^* such that $\frac{w^*}{2} = \lambda\,|_{\lambda\le .5},\ (1-\lambda)\,|_{\lambda>.5}$, and

$$t_T(\lambda,T) \sim N\left(0, \left(12\sigma^2\Phi\right)^{1/2}\lambda^{**}\right);\ \lambda^{**} = 1/\left(w^{**}+3\right)$$

where w^{**} is a standard flattop window. Clearly, both distributions heavily hinge on σ and λ but not on the sample size. Moreover, the values reported are approximations of the true values obtained by numerical experimentation, which are exhibited in Table 2 together with the extreme values of eqs. (8.1) and (8.2).

As an exercise, after dropping henceforth for ease of reading the notation λ, suppose now that the alternative I(0) non-break model with constant and trend were given by

A.3) $$\Delta y_t = \bar{\mu}_1 + \bar{\tau}_1 t + \varepsilon_t$$

so that, for $\varepsilon_t \sim I.I.D.(0,\sigma^2)$, the coefficients' limit distributions are $T^{1/2}(\hat{\mu}_1 - \mu_1^*) \sim N(0,4\sigma^2)$ and $T^{3/2}(\hat{\tau}_1 - \tau_1^*) \sim N(0,12\sigma^2)$.

The variances of $\hat{\mu}_1$ and $\hat{\tau}_1$ are lower than their break counterparts derived from eq. (A.2), since they are: $4\sigma^2$ and $12\sigma^2$ vs. $4\sigma^2/\lambda$ and $12\sigma^2/\lambda^3$, respectively. By consequence their standard errors are also smaller.

The standard *t* statistics of eq. (A.3), respectively denoted as $t_T^*(L)$ and $t_T^*(T)$ are

A.3.1) $$t_T^*(L) = -\left(W(1) - 3\int_0^1 W(r)dr\right)$$

A.3.2) $$t_T^*(T) = 3^{1/2}\left(W(1) - 2\int_0^1 W(r)dr\right),$$

which respectively correspond to those of eqs. A.2.1 and A.2.2 if $\lambda = 1$. They are smaller than these and of those reported in eqs. (8.1) and (8.2). Incidentally, for both statistics to be asymptotically equal to the standard value of 1.96, the 95% fractile values of *W(1)* and $\int_0^1 W(r)dr$ must respectively equal 7.31 and 3.09.

The coefficients of eq. (A.3) are:

$$\bar{\mu}_1 = -2\left(W(1) - 3\int_0^1 W(r)dr\right),\ \bar{\mu}_2 = 6\left(W(1) - 2\int_0^1 W(r)dr\right)$$

which may be confronted with those of eq. (A.2):

$$\mu_1 = -2\left(\lambda W(1) - 3\int_0^1 W(r)dr\right)\Big/\lambda,\ \mu_2 = 6\left(\lambda W(1) - 2\int_0^1 W(r)dr\right)\Big/\lambda^2.$$

If $\lambda = 1$, $\bar{\mu}_1 = \mu_1$ and $\bar{\mu}_2 = \mu_2$. Instead, for $\lambda \to 0$, $\bar{\mu}_1 < \mu_1$ and $\bar{\mu}_2 < \mu_2$, namely, the coefficients of the non-break alternative model are smaller than those of the break model, especially if the true breaks occur at early dates.

As a further exercise, we assume now that the alternative I(0) model is made of the two breaks only , i.e.

A.4) $$\Delta y_t(\lambda) = \mu_2 DU_t(\lambda) + \tau_2 DT_t(\lambda) + \varepsilon_t(\lambda)$$

The resulting *t* statistics, respectively denoted as $t_T^{**}(\lambda,L)$ and $t_T^{**}(\lambda,T)$, are

A.4.1) $$t_T^{**}(\lambda, L) = \frac{\left((1+2\lambda)W(1) - 3\int_0^1 W(r)dr\right)}{(1-\lambda)^{1/2}}$$

A.4.2) $$t_T^{**}(\lambda, T) = 3^{1/2}\frac{\left((1+\lambda)W(1) - 2\int_0^1 W(r)dr\right)}{(1-\lambda)^{1/2}}$$

which correspond to those of eqs. (A.3.1) and (A.3.2), respectively, if $\lambda = 0$.

Finally, if the disturbance ε_t in eq. (2) is *I*(1) as in Perron and Zhu (2005), then eq. (6) is

$$\Theta_T(\lambda) = \begin{bmatrix} 2\lambda/15 & -1/10 & -\lambda/30 & 1/10 \\ & 6/5\lambda & -1/10 & -6/5\lambda \\ & & 2/15 & 0 \\ & & & \dfrac{6}{5\lambda(1-\lambda)} \end{bmatrix}$$

whereby the *t*-statistics of the breaks, the counterparts of eqs. (8.1) and (8.2), are given by the following

A.5.1) $$t_T(\lambda, L) = 3\frac{30^{1/2}\left(\lambda W(1) - \int_0^1 W(r)dr\right)}{\lambda(\lambda-1)}$$

A.5.2) $$t_T(\lambda, T) = 30\frac{\lambda(3\lambda-1)W(1) - 2(2\lambda-1)\int_0^1 W(r)dr}{\lambda(\lambda-1)\left[30\lambda(1-\lambda)\right]^{1/2}}$$

which are, for the same values of λ, distinctively larger than their I(0) counterparts, reflecting the spuriousness of the equation they are derived from.

Appendix 2

PCA, PFA and True Factor Number Selection

Let $\mathrm{X}_t : (T \times K)$ as defined in Sect. 3.1. By virtue of the common-component static PFA model (Chamberlain and Rothschild, 1983) the matrix X_t can be rewritten as

A.6) $$\mathrm{X}_t = F_t C' + V_t$$

where $F_t : (T \times r)$ is the factor matrix and $C : (K \times r)$ is the matrix of factor loadings. The true number *r* of factors is unknown ex ante and can be endogenously determined by formal statistical procedures characterized by information criteria that minimize, under penalization, the variance $\Psi_t = V_t ' V_t$, where $V_t : (T \times K)$ is the idiosyncratic component matrix (Bai and Ng, 2002, 2007). X_t is observed, while the other variables and the loadings are unobserved.

Specifically, the following hold: $F_t ' F_t = I_r$ and $F_t F_t '/ K = \Xi : (K \times K)$, which is p.s.d., and. $\text{m.e.}(C'C/K), \text{m.e.}(\Psi/K), \text{m.e.}(\Xi/TK) \to 0$ as $T, K \to \infty$, where m.e. is the maximum eigenvalue of the given matrix and is employed to gauge the magnitude of a matrix. For *K* fixed and $T \to \infty$, the first magnitude converges to a constant and the other two toward zero as above.

The symmetric asymptotic covariance matrix of eq. (A.6) is

A.7) $$\mathrm{X}_t\,'\mathrm{X}_t/\mathrm{T} = CF_t\,'F_tC' + \Psi_t$$

whose first component matrix, by virtue of the Spectral Decomposition Theorem equals ERE, where $\mathrm{R}:(K \times K)$ is the diagonal matrix of the eigenvalues, and $\mathrm{E}:(K \times K)$ is the eigenvector matrix (Sect. 3.3). Then: $C = \mathrm{ER}^{1/2} = (\mathrm{X}_t F_t / K)'$ which are the PCA scores. In PFA, the estimated common components (or factor scores) are $\hat{C}_t = (F_t C)'$, where $\hat{C}_t : (K \times T)$ and $V_t = \mathrm{X}_t - \hat{C}_t\,'$. The PCA scores are mutually orthogonal but cannot be used to estimate V_t for small *T* since they provide no minimal Ψ_t. On the contrary, factor scores can be used to estimate V_t even for small *T* but are correlated among them since $\mathrm{corr}(\hat{C}_t) \to \infty$ as $T, K \to \infty$, whereas $\mathrm{corr}(\hat{C}_t) = \mathrm{op}(1)$ for $T \to \infty$ and *K* fixed.

The formal statistical procedures reported by Bai and Ng (2002) and utilized to compute the true number of common factors (*r*) are eight in total, namely, three "Panel Criteria" (PC), three "Information Criteria" (IC), and adjusted versions of the Akaike and Bayesian Information Criteria (AIC and BIC). Of these, one only is selected in the present context for ease of space and also because it makes no direct use of the matrix Ψ_t in the penalty function.

Let $k_{\max}$ be the maximum number of factors admitted, usually 8, and the sequence $k = 1, ..., k_{\max}$. Let $\hat{v}_{i,j}$, $i \in T$, $j \in K$, the *i*th and *j*th element of matrix V_t, then

A.8) $$V(k) = \min\left(TK^{-1}\sum_{i=1}^{T}\sum_{j=1}^{K}\hat{v}_{i,j}^2\right)$$

is a scalar variance indicator found for each *k*. The information criterion reported is based on detecting the minimum value of $V(k)$ plus a penalty for overfitting within the *k* sequence:

A.9) $$IC = \ln V(k) + k\left(\frac{T+K}{TK}\right)\ln\left(\frac{TK}{T+K}\right).$$

where *IC* is a $k_{\max}$-sized vector wherein to find the minimal *IC* and detect the associated value of *k* that corresponds to the true number *r* of factors. Other things equal, the penalty term tends to zero as $T, K \to \infty$ and to a constant value for $T \to \infty$ and *K* fixed. For $\hat{v}_{i,j} \sim N.I.D.(0,1)$ *IC* increases as $k \to k_{\max}$ independent of the magnitude of *T* and *K*, specifically: $IC \to \alpha$ where $0 < \alpha < 1$. In addition, for any given *k*, $IC \to 0$ for $T, K \to \infty$ and $IC \to \alpha$ for $T \to \infty$ and *K* fixed. In practice, the selection procedure involved by eq. (A.9) favors in the vast majority of cases a small number of factors *k* and is asymptotically efficient for $T, K \to \infty$.

Endnotes

---

[1] The empirical distribution of the two simulated *t* statistics is a standard Normal with positives and negatives entering with equal probability weights. Obviously, they retain the property of being equal to the square-rooted Wald statistics for testing the zero value of the corresponding coefficient. Their variances are further discussed and shown in Table 2.

[2] By construction, the squares of the two *t* statistics, for given λ, correspond to their respective limit Wald-test statistics. As for the first of them, see for instance Bai and Perron (2003). For both, see Vogelsang (1999) although the simulation method adopted therein differs from that of the present paper.

[3] The procedure for computing the critical values and other specifics included in Table 2 is reliable and fast in a Matlab environment, even for large *N*. For *N*=10,000 it takes no more than 3 mins. and 40 secs. on a standard PC with a 4 Gb. RAM. The code is available upon request to the author.

[4] Although unreported for ease of space, Montecarlo simulations of eqs. (8.1) and (8.2) were performed also for *T*=100,300 and 500 producing very similar critical values as those reported in Table 1. Therefore, such values are independent of *T*.

[5] The model of eqs. (9.1) - (9.2) for expositional simplicity presupposes no exogenous regressors. The expectation that matrix Π be of full rank presupposes instead instrument relevance. Both assumptions are customarily the object of empirical testing, see e.g. Kleibergen (2005), Kleibergen and Mavroeidis (2009).

[6] By means of some applied experimenting with Montecarlo simulation, it is shown that in a standard OLS (*T*=200) model with an I(0) endogenous variable and $T \geq K \geq 1$ regressors, the *t* statistics of the coefficients of the deterministic components, by departing from values below unity at *K*=1, diverge toward a value of 2.00 at a rate of $K^{1/6}$. With an I(1) endogenous variable, the same *t* statistics depart at *K*=1 from values over 8.0 and 15.0 for the constant and the trend, respectively, and are op(1) for increasing *K*.

[7] Selection of the appropriate instruments is usually costly and lengthy and often unsatisfactory, since exogeneity and relevance must be synchronously met. In fact, the procedure of throwing away the instruments that do not meet this requirement (e.g. by using partial F statistics as suggested by Stock and Wright, 2000) may end up with obtaining the undesirable result $L < K$.

[8] Pivotality (Kleibergen, 2002) implies that parameter inferences are independent of the reduced-form parameters. Statistical invariance establishes that parameter inferences remain unchanged when the IVs are subjected to one-to-one measurable transformations, e.g. changing their order of appearance. Similarity implies that the distribution of a test statistic does not vary if its related parameter is made to vary within a given hypothesis set of values.

[9] The bias arises when there is endogeneity in the linear model, i.e. when moments and their derivatives (the Jacobian matrix elements) are not zero correlated. The bias increases in magnitude by a factor given by the number of instruments (Newey and Smith, 2004; Newey and Windmeijer, 2009).

[10] Regressor endogeneity in eq. (9.1) cannot be tested by simply verifying the correlation or covariance between forcings and the structural error, since it is zero by construction. Granger causality testing between these variables is definitely more appropriate.

[11] This feature allows eq. (9.1) to belong to the class of partial structural change models as envisaged, for instance, by Bai and Perron (2003).

[12] The 4th Assessment Report (AR4, 2007) makes use of spurious techniques (see Sect. 3.1) to estimate the trending behavior of temperatures over the past 150 years and derives methodologically ungrounded conclusions, shared with Nobel Peace Prize Al Gore's statements (e.g. the Capitol Hill testimony on global warming in March 2007).

[13] On the subtle, yet very significant difference between climate and temperatures see Baliunas and Soon (2003). In addition, global warming and climate change are currently used interchangeably, although recently the first definition has become less popular among common media.

[14] By dating back to 1850, this data subset – albeit limited – is the only available in Maddison's comprehensive statistics that stretches the period chosen.

[15] All level forcings are loggable, exclusion made for some volcanic activity variables (VOL, VOLSOL and COMPVOL) which come in negatives. In such case the raw data were used. The smoothing parameter of the HP filter, given annual observations, was chosen to be 6.25, which is the value suggested by Ravn and Uhlig (2001). The motivation of this choice stands in the results obtained after using different smoothing values (100 and 400) and the standard centering and scaling procedure in alternative regression runs of the endogenous variable. In all cases, significant residual autocorrelation and high standard errors of estimation ensued, this not being the case with the selected smoother as shown in Table 3.

[16] First-order autocorrelation of the structural residuals is low with the prefered smoothing factor, as it never exceeds 0.05. It is also similarly low, but at times much higher, in the cases of HP filtering of the dataset with smoothing factors of 100 and 400. Worse results hold for centering and scaling, and even more so for first differencing, which produce autocorrelation coefficients in general no lower than 0.10-0.15 for all of the alternative model specifications. Instead, ARCH(1) testing rejects heteroskedasticity at the 5% level in most cases and behaves better than the prefered smoothing factor, where rejection requires a much higher level. It should be remarked, however, that detected heteroskedasticity can be easily disposed of in GMM estimation, while in that context autocorrelation always constitutes a serious problem.

[17] The logged levels and first differences (Δ) of the BEA time series can best be represented by the following equations:

$$Log(\text{BEA})_t = \underset{(6.4)}{1.103} - \underset{(2.1)}{12^{-3}T} + \underset{(3.9)}{10^{-6}T^2} + \underset{(8.8)}{.578Log(\text{BEA})_{t-1}};\ \text{R}^2 = .829,\ \text{DW}=1.981$$

$$\Delta Log(\text{BEA})_t = \underset{(6.3)}{-1.093} + \underset{(1.7)}{10^{-3}T} - \underset{(3.4)}{10^{-6}T^2} + \underset{(6.3)}{.418Log(\text{BEA})_{t-1}};\ \text{R}^2 = .209,\ \text{DW}=1.984$$

where the coefficients' *t*-statistics are reported in brackets, and T and T^2 respectively are the linear and the squared trend. DW is Durbin-Watson's standard test statistic. Although apparently spurious, both equations indicate a tendency of mean world temperatures to taper off overtime. In fact the logged levels significantly fall at a rising pace while their first differences rise at a decreasing pace. However, the reported effects are small since for instance, *coeteris paribus*, the absolute temperature levels would take over one eighty years to fall by 1% from now.

[18] According to some IPPC estimates, "a GHG level of 650 ppm would "likely" warm the global climate by around 3.6°C, while 750 ppm would lead to a 4.3°C warming, 1,000 ppm to 5.5°C and 1,200 ppm to 6.3°C. Future GHG concentrations are difficult to predict and will depend on economic growth, new technologies and policies and other factors" (Press conference, Paris, February 2, 2007)

[19] As to the Zivot-Andrews single-break and UR test, the dates of 1875 and 1877 are selected depending on the lags included in the endogenous variable. As to the Bai-Perron multiple-breaks test, which is set to allow a maximum of four level breaks, there is a large multiplicity of level breaks depending on the lags attributed to the entirety of the forcings. By sticking to the lowest BIC among these alternatives, the break dates range from 1874 to 1975, passing through the Fifties and the Sixties.

[20] The minima of the level and of the trend breaks respectively are -5.2086 and -2.5382, located in the years 1980-81, while the respective maxima are 3.4758 and 4.5458, located in the years 1870 and 1982. All of these values are associated to extrema of λ and are nonsignificant by the standards established in Table 1.

[21] The original weighted shares exhibit small jags derived from the corresponding coefficients. For ease of inspection, they are trended by means of HP filtering with a smoothing coefficient equal to 400, consistent with yearly observations and large enough to produce the continuous lines shown in the graphs.

References

Abdussamatov H. (2004) *About the Long-Term Coordinated Variations of the Activity, Radius, Total Irradiance of the Sun and the Earth's Climate*, International Astronomical Union, DOI: 10.1017/S1743921304006775, 541-542.

Alanko-Huotari, K., I.G. Usoskin, K. Mursula, and G.A. Kovaltsov (2006) *Global Heliospheric Parameters and Cosmic Ray Modulation: an Empirical Relation for the Last Decades*, Solar Physics, 238, 391-404.

Alley R.B. (2000) *The Younger Dryas Cold Interval as Viewed from Central Greenland*, Quaternary Science Reviews, 19, 213-226.

Ammann, C.M. and Naveau P. (2003) *Statistical analysis of tropical explosive volcanism occurrences over the last 6 centuries*, Geophysical Research Letters, 30, No. 5, 1210, DOI:10.1029/2002GL016388.

Anatolyev S. and Gospodinov N. (2010) *Specification Testing in Models with Many Instruments*, Econometric Theory, forthcoming.

Anderson T.W. and Rubin H. (1949) *Estimation of the Parameters of a Single Equation in a Complete System of Stochastic Equations*, The Annals of Mathematical Statistics, 20, 46-63.

Anderson T.W. (1984) *An Introduction to Multivariate Statistical Analysis*, Wiley, New York.

Andrews D.W.K. (1993) *Tests for Parameter Instability and Structural Change with Unknown Change Point*, Econometrica, 61, 821-856.

Andrews D.W.K., Moreira M. and Stock J.H. (2006) *Optimal Two-Sided Invariant Similar Tests for Instrumental Variable Regression*, Econometrica, 74, 715-752.

Andrews D.W.K. and Stock J.H. (2007) *Testing With Many Weak Instruments*, Journal of Econometrics, 138, 24-46.

Bai J. and Ng S. (2002) *Determining the Number of Factors in Approximate Factor Models*, Econometrica, 70, 191-221.

Bai J. and Ng S. (2007) *Determining the Number of Primitive Shocks in Factor Models*, Journal of Business and Economic Statistics, 25, 52-60.

Bai J. and Ng S. (2008) *Instrumental Variable Estimation in a Data Rich Environment*, Econometric Theory, Forthcoming.

Bai J. and Perron P. (2003) *Computation and Analysis of Multiple Structural Change Models*, Journal of Applied Econometrics, 18, 1-22.

Baliunas S. and Soon W. (2003) *Lessons and Limits of Climate History: Was the 20th. Century Climate Unusual?*, The George C. Marshall Institute, Washington D.C..

Banerjee A., Lumsdaine R.L. and Stock J.H. (1992) *Recursive and Sequential Tests of the Unit-Root and Trend-Break Hypotheses: Theory and International Evidence*, Journal of Business and Economic Statistics, 10, 271-287.

Bard, E., G. Raisbeck, F. Yiou, and J. Jouzel (2000) *Solar irradiance during the last 1200 years based on cosmogenic nuclides*, TELLUS B, 52, pp. 985-992.

Bard E. and Frank M. (2006) *Climate Change and Solar Variability: What's new Under the Sun?*, Earth and Planetary Science Letters, 248, 1-14.

Brohan P., Kennedy J.J., Harris I., Tett S.F.B. and Jones P.D. (2006) *Uncertainty Estimates in Regional and Global Observed Temperature Changes: a new Dataset from 1850*, Geophysical Research, 111, DOI:10.1029/2005JD006548.

Bürger G., (2007) *Comment on "The Spatial Extent of 20th-Century Warmth in the Context of the Past 1200 Years"*, Science, 316/5833, 1844.

Chamberlain G. and Rothschild M. (1983) *Arbitrage, Factor Structure, and Mean-Variance Analysis on Large Asset Markets*, Econometrica, 51, 1281-1304.

Chenet A.L., Fluteau F. and Courtillot V. (2005) *Modeling Massive Sulphate Aerosol Pollution Following the Large 1783 Laki Basaltic Eruption*, Earth and Planetary Science Letters, 236, 721-731.

Clarida R., Galì J. and Gertler M. (2000) *Monetary Policy Rules and Macroeconomic Stability: Evidence and Some Theory*, The Quarterly Journal of Economics, CXV, 147-180.

Cragg J.G. and Donald S.G. (1993*) Testing Identifiability and Specification in Instrumental Variable Models*, Econometric Theory, 9, 222-240.

Crowley, T.J. (2000) *Causes of Climate Change Over the Past 1000 Years*, Science, 289, 270-277.

Cruz L.M. and Moreira M.J. (2005) *On the Validity of Econometric Techniques with Weak Instruments*, The Journal of Human Resources, XL, 393-410.

Cullen, H.M., deMenocal, P.B., Hemming, S., Hemming, G., Brown, F.H., Guilderson, T. and Sirocko, F. (2000) *Climate Change and the Collapse of the Akkadian Empire: Evidence from the Deep Sea*, Geology, 28, 379-382.

Dickey D.A. and Fuller W.A. (1979*) Distribution of the Estimators for Autoregressive Time Series With a Unit Root*, Journal of the American Statistical Association, 74, 427-431.

Doran P.T. and Zimmerman M.K. (2009) *Examining the Scientific Consensus on Climate Change*, Transactions of the American Geophysical Union, 90, No.3.

Engle R.F. (1982) *Autoregressive Conditional Heteroskedasticity with Estimates of the Variance of UK Inflation*, Econometrica, 50, 987-1008.

Esper J. and Frank D. (2009) *The IPCC on a heterogeneous Medieval Warm Period*, Climatic Change, 94, 267–273

Fouka P., Fröhlich C., Spruit H. and Wigley T.M. (2006) *Variations in Solar Luminosity and their Effect on the Earth's Climate*, Nature, 443, 161-166.

Gill, R.B. (2000) *The Great Maya Droughts: Water, Life, and Death*, University of New Mexico Press, Albuquerque.

Granger C.W.J. (1969) *Investigating Causal Relations by Econometric Models and Cross-Spectral Models*, Econometrica, 37, 424-438.

Granger C.W.J. and Newbold P. (1974) *Spurious Regressions in Econometrics*, Journal of Econometrics, 2, 111-120.

Granger C.W.J., Namwon H. and Jeon Y. (2001) *Spurious Regressions with Stationary Series*, Applied Economics, 33, 899-904.

Gray W.M., Sheaffer J.D. and Landsea C.W. (1997) *Climate Trends Associated with Multidecadal Variability of Atlantic Hurricane Activity*, in Diaz H.F. and Pulwarty R.S. eds., *Hurricanes: Climate and Socioeconomic Impacts*, Springer-Verlag, New York, N.Y., 15-53.

Hansen B. E. (2000) *Testing for Structural Change in Conditional Models*, Journal of Econometrics, 97, 93-115.

Hansen B.E., Heaton J. and Yaron A. (1996) *Finite Sample Properties of Some Alternative GMM Estimators*, Journal of Business and Economic Statistics, 14, 262-80.

Hansen B.E. and West K.D. (2002) *Generalized Method of Moments and Macroeconomics*, Journal of Business and Economic Statistics, 20, 460-469.

Hansen J., Sato M., Kharecha P., Russell G., Lea D.W. and Siddall M. (2007) *Climate Change and Trace Gases*, Philosophical Transactions of the Royal Society, 365, 1925–1954.

Hansen L.P. (1982) *Large Sample Properties of Generalized Method of Moments Estimator*, Econometrica, 50, 1029-1054.

Hodrick, R., and E.P. Prescott, (1997) *Postwar Business Cycles: An Empirical Investigation*, Journal of Money, Credit and Banking, 29, 1–16

Kaufmann R.K., Kauppi H. and Stock J.H. (2006) *Emissions, Concentrations and Temperature: A Time Series Analysis*, Climatic Change, in review.

Kiefer N.M. and Vogelsang T.J. (2002) *Heteroskedasticity-Autocorrelation Robust Testing Using Bandwidth Equal to Sample Size*, Econometric Theory, 18, 1350-66.

Kim D. and Lee Y. (2009) *Likelihood Ratio based Joint Test for the Exogeneity and the Relevance of Instrumental Variables*, mimeo.

Kim D. and Perron P. (2009) *Unit Root Tests Allowing for a Break in the Trend Function at an Unknown Time under Both the Null and Alternative Hypotheses*, Journal of Econometrics, 148, 1-13.

Kleibergen, F. (2002) *Pivotal Statistics for Testing Structural Parameters in Instrumental Variables Regression*, Econometrica, 70, 1781-1803.

Kleibergen, F. (2005) *Testing Parameters in GMM without Assuming that they are Identified*, Econometrica, 73, 1103-1124.

Kleibergen, F. (2008) *Testing*, New Palgrave Dictionary of Economics, Edited by Durlauf S.N. and Blume L.E., Second Edition.

Kleibergen F. and Mavroeidis S. (2009) *Weak Instrument Robust Tests in GMM and the New Keynesian Phillips Curve*, Journal of Business and Economic Statistics, 27, 293-311.

Kleibergen F. and Paap R. (2007) *Generalized Reduced Rank Tests using the Singular Value Decomposition*, Journal of Econometrics, 139, 181-216.

Krivova N.A., Balmaceda L. and Solanki S.K. (2007) *Reconstruction of solar total irradiance since 1700 from the surface magnetic flux*, Astronomy & Astrophysics, 467, 335–346.

Lanne M. and Liski M. (2004) *Trends and Breaks in Percapita Carbon Dioxide Emissions, 1870-2029*, The Energy Journal, 25, 41-65.

Lean, J. (2000) *Evolution of the Sun's Spectral Irradiance since the Maunder Minimum*, Geophysical Research Letters, 27, 16, 2425-2428.

Lean, J. (2004) *Solar Irradiance Reconstruction*, IGBP PAGES/World Data Center for Paleoclimatology, Data Contribution Series No. 2004-035, NOAA/NGDC Paleoclimatology Program.

Maddison A. (2007) *The Contours of the World Economy 1-2030 AD*, Oxford University Press, Oxford, U.K.

Mann, M.E., Cane M.A., Zebiak S.E., and Clement A. (2005*) Volcanic and Solar Forcing of the Tropical Pacific over the Past 1000 Years*, Journal of Climate, 18, 417-456.

Marland G., Boden T.A. and Andres R.J. (2007) *Global, Regional, and National CO2 Emissions. In Trends: A Compendium of Data on Global Change*, Carbon Dioxide Information Analysis Center, Oak Ridge National Laboratory, U.S. Department of Energy, Oak Ridge, Tenn., U.S.A.

McDonald G.M. and Case R.A. (2005) *Variations in the Pacific Decadal Oscillation over the Past Millennium*, Geophysical Research Letters, 32, L08703, doi:10.1029/2005GL022478.

Mikusheva A., (2007) *Robust Confidence Sets in the Presence of Weak Instruments*, MIT, Department of Economics, Working Paper No. 07-27.

National Geophysical Data Center (NGDC, 2007) *Tables of Monthly Sunspot Numbers 1700-Present*, NOAA Satellite and Information Service.

Newey W. and West K. (1987) *A Simple Positive-Definite Heteroskedasticity and Autocorrelation Consistent Covariance Matrix*, Econometrica, 55, 703-708.

Newey W. and Smith R.J. (2004) *Higher Order Properties of GMM and Generalized Empirical Likelihood Estimators*, Econometrica, 72, 219-255.

Newey W. and Windmeijer F. (2009) *GMM with Many Weak Moment Conditions*, Econometrica, 77, 687-719.

Noriega A. E. and Ventosa-Santaulària N. (2005) *Spurious Regression under Broken Trend Stationarity*, School of Economics, University of Guanajuato, Working Paper EM-0501.

Perron P. (1989) *The Great Crash, the Oil Price Shock, and the Unit Root Hypothesis*, Econometrica, 57, 1361-1401.

Perron P. (1997) *Further Evidence on Breaking Trend Functions in Macroeconomic Variables*, Journal of Econometrics, 80, 335-385.

Perron P. and Yabu T. (2009*) Estimating Deterministic Trends with an Integrated or Stationary Noise Component*, Journal of Econometrics, 151, 56-69.

Perron P. and Zhu X. (2005) *Structural Breaks with Deterministic and Stochastic Trends*, Journal of Econometrics, 129, 65-119.

Phillips P.C.B. (1986) *Understanding Spurious Regressions in Econometrics*, Journal of Econometrics, 33, 311-340.

Ravn M.O. and Uhlig H. (2001) *On Adjusting the HP-Filter for the Frequency of Observations*, LBS Department of Economics, Working Paper No. DP (2001)/1.

Rind D., Lean J., Lerner J., Lonergan P. and Leboissitier A. (2008) *Exploring the stratospheric/tropospheric response to solar forcing*, Journal of Geophysical Research, 113, DOI:10.1029/2008JD010114.

Robertson A., Overpeck J., Rind D., Mosley-Thompson E., Zielinski G., Lean J., Koch D., Penner J., Tegen I., and Healy R. (2001) *Hypothesized Climate Forcing Time Series for the Last 500 Years*, Journal of Geophysical Research, 106, 14,783-14,803.

Shaviv N. (2005) *On Climate Response to Changes in the Cosmic Ray Flux and Radiative Budge*t, Journal of Geophysical Research, 110, 1-15.

Shaviv N. and Veizer J. (2003) *Celestial Driver of Phanerozoic climate?,* GSA Today, 13, 4-10.

Shen C., Wang W.C., Gong W. and Hao Z. (2006) *A Pacific Decadal Oscillation Record since 1470 AD Reconstructed from Proxy Data of Summer Rainfall over Eastern China*, Geophysical Research Letters, 33, L03702.

Shindell D.T., Schmidt G.A., Mann E.M. and Faluvegi G. (2004) *Dynamic Winter Climate Response to Large Tropical Volcanic Eruptions since 1600*, Journal of Geophysical Research, 109, D05104, 1-12.

Smith R.J. (2005) *Automatic Positive Semidefinite HAC Covariance Matrix and GMM estimation*, Econometric Theory, 25, 158-70.

Solanki S.K., Usoskin I.G., Kromer B., Schüssler M. and Beer J. (2004) *Unusual Activity of the Sun During Recent Decades Compared to the Previous 11,000 Years*, Nature, 431, 1084 - 1087.

Staiger D. and Stock J.H. (1997) *Instrumental Variables Regression with Weak Instruments*, Econometrica, 65, 557-86.

Stern D. I. (2002) *Explaining Changes in Global Sulfur Emissions: an Econometric Decomposition Approach*, Ecological Economics 42, 201-220.

Stern D.I. (2004) *A Multicointegration Model of Global Climate Change*, Rensselaer Working Papers in Economics, No. 0406.

Stock J.H. and Wright J. (2000) *GMM with Weak Identification*, Econometrica, 68, 1055-1096.

Stock J. H., Yogo M. and Wright J. (2002) *A Survey of Weak Instruments and Weak Identification in Generalized Method of Moments*, Journal of Business and Economic Statistics, 20, 518-529.

Stock J.H. and Yogo M. (2003) *Testing for Weak Instruments in Linear IV Regression*, Department of Economics, Harvard University.

Sun Y. (2004) *A Convergent t-statistic in Spurious Regressions*, Econometric Theory, 20, 943-962.

Sun, Y., Phillips P.C.B. and Jin S. (2008) *Optimal Bandwidth Selection in Heteroskedasticity-Autocorrelation Robust Testing*, Econometrica 76, 175-94.

Svensmark H. (1998) *Influence of Cosmic Rays on Earth's Climate*, Physical Review Letters, 81, 5027-5030.

Svensmark, H. and Frijs-Christensen, E. (2007) Reply *to Lockwood and Fröhlich. The Persistent Role of the Sun in Climate Forcing*, Danish National Space Center Scientific Report 3/(2007).

Trouet, V., Esper J., Graham N.E., Baker A., Scourse J.D. and Frank D.C. (2009) *Persistent Positive North Atlantic Oscillation Mode Dominated the Medieval Climate Anomaly*, Science, 324, 78-80.

Usoskin I.G., Mursula K., Solanki S., Schüssler M. and Kovaltsov G.A. (2003) *A Physical Reconstruction of Cosmic Ray Intensity since 1610*, Journal of Geophysical Research, 107, SSH 13, 1-6.

Usoskin I.G., Mursula K., Solanki S., Schüssler M. and Alanko K. (2004a) *Reconstruction of Solar Activity for the Last Millennium using* ^{10}Be *Data*, Astronomy and Astrophysics, 413, 745-751.

Usoskin I.G., Mursula K., Solanki S., Schüssler M. and Alanko K. (2004b) *Millennium-Scale Sunspot Number Reconstruction: Evidence for an Unusually Active Sun since the 1940s*, Physical Review Letters, 91, 211101:1-4.

Usoskin I.G., Solanki S.K. and Korte M. (2006) *Solar Activity Reconstructed over the Last 7000 years: The Influence of Geomagnetic Field Changes*, Geophysical Research Letters, 33, L08103, 1-4.

Vogelsang T.J. (1997) *Wald-Type Tests for Detecting Breaks in the Trend Function of a Dynamic Time Series*, Economic Theory, 13, 818-849.

Vogelsang T.J. (1999) *Testing for a Shift in Trend when Serial Correlation is of Unknown Form, Tinbergen Institute of Econometrics*, Discussion Paper No. TI99-016/4.

Vogelsang T.J. and Perron P. (1998) *Additional Tests for a Unit Root Allowing for a Break in the Trend Function at an Unknown Time*, International Economic Review, 39, 1073-1100.

Yogo M. (2004*) Estimating the Elasticity of Intertemporal Substitution when Instruments are Weak*, Review of Economics and Statistics, 86, 797–810.

Zivot E. and Andrews D.W.K. (1992) *Further Evidence on the Great Crash, the Oil-Price Shock,* *and the Unit-Root Hypothesis*, Journal of Business and Economic Statistics, 10, 251-270.

Table 1

Absolute critical values of $t_T(\lambda, L)$ and $t_T(\lambda, T)$, eqs. (8.1) and (8.2), for select magnitudes of λ and different marginal significance levels (bold) with upper (<) and lower (>) 10% confidence bands. *T*=200*.

	<	**1%**	>	<	**5%**	>	<	**10%**	>
					λ =0.10				
$t_T(\lambda, L)$	12.18	**11.53**	10.88	8.88	**8.23**	7.58	7.16	**6.51**	5.86
$t_T(\lambda, T)$	14.50	**13.73**	12.97	10.41	**9.64**	8.88	8.29	**7.52**	6.76
					λ =0.20				
$t_T(\lambda, L)$	8.14	**7.73**	7.32	5.67	**5.26**	4.85	4.53	**4.12**	3.71
$t_T(\lambda, T)$	9.43	**8.94**	8.44	6.64	**6.15**	5.65	5.28	**4.79**	4.29
					λ =0.30				
$t_T(\lambda, L)$	5.45	**5.15**	4.85	4.08	**3.78**	3.48	3.21	**2.91**	2.61
$t_T(\lambda, T)$	6.81	**6.46**	6.11	4.81	**4.46**	4.11	3.84	**3.49**	3.14
					λ =0.40				
$t_T(\lambda, L)$	4.78	**4.53**	4.28	3.42	**3.17**	2.92	2.70	**2.45**	2.20
$t_T(\lambda, T)$	4.98	**4.72**	4.45	3.58	**3.31**	3.05	2.82	**2.55**	2.29
					λ =0.50				
$t_T(\lambda, L)$	4.38	**4.15**	3.91	3.18	**2.94**	2.71	2.54	**2.31**	2.08
$t_T(\lambda, T)$	4.18	**3.95**	3.72	3.16	**2.93**	2.70	2.51	**2.27**	2.04
					λ =0.60				
$t_T(\lambda, L)$	4.44	**4.20**	3.95	3.25	**3.01**	2.77	2.63	**2.38**	2.14
$t_T(\lambda, T)$	4.96	**4.70**	4.44	3.60	**3.34**	3.08	2.86	**2.60**	2.34

				λ =0.70					
$t_T(\lambda, L)$	5.83	**5.53**	5.23	4.02	**3.72**	3.42	3.22	**2.92**	2.62
$t_T(\lambda, T)$	6.75	**6.40**	6.05	4.73	**4.38**	4.03	3.77	**3.42**	3.07
				λ =0.80					
$t_T(\lambda, L)$	7.82	**7.41**	7.00	5.60	**5.19**	4.78	4.37	**3.96**	3.56
$t_T(\lambda, T)$	9.30	**8.81**	8.32	6.66	**6.17**	5.68	5.19	**4.70**	4.21
				λ =0.90					
$t_T(\lambda, L)$	11.78	**11.13**	10.48	8.86	**8.21**	7.56	7.02	**6.37**	5.72
$t_T(\lambda, T)$	13.97	**13.20**	12.44	10.43	**9.66**	8.89	8.27	**7.50**	6.73

* The marginal significance levels (1%,5% e 10%) represent the unit complements of the fractiles (99%, 95% and 90%) of the distribution of the *t* statistic of an artificial Random Walk of *N*=10,000 MC replications. The confidence bands are obtained by applying 2 standard deviations.

Table 2

Descriptive statistics of the *t* statistic of a break in level $t_T(\lambda, L)$, eq. (8.1), and of the *t* statistic of a break in trend $t_T(\lambda, T)$, eq. (8.2). 1,000 MC draws of eq. (1) for sample size *T*=200 and break fractions $0.10 \le \lambda \le 0.90$,1% and 99% fractiles.

λ	**mean**	**variance**	**minimum**	**maximum**	**1%**	**99%**
			Break in level			
0.10	-0.349	23.999	-14.997	17.091	-12.092	10.741
0.20	0.097	8.741	-8.996	9.256	-6.551	6.922
0.30	-0.033	5.300	-6.859	7.883	-5.250	5.448
0.40	-0.062	3.740	-5.883	8.370	-4.459	4.510
0.50	-0.074	2.997	-5.769	4.994	-4.201	4.046
0.60	0.047	3.567	-5.678	6.095	-4.100	4.257
0.70	0.035	5.833	-7.211	7.107	-5.873	5.524
0.80	0.033	11.027	-11.912	10.705	-7.931	8.133
0.90	-0.080	24.705	-14.462	15.300	-10.645	11.589
			Break in trend			
0.10	0.429	33.599	-19.937	17.487	-12.812	14.235
0.20	-0.146	12.560	-10.966	11.162	-8.480	7.605
0.30	0.092	7.349	-9.005	8.430	-6.312	6.260
0.40	0.080	4.167	-7.438	6.544	-4.745	5.011
0.50	0.010	2.759	-5.396	5.571	-3.542	4.138
0.60	0.082	3.917	-6.432	7.589	-4.770	4.665
0.70	0.036	8.153	-9.421	8.600	-6.149	6.888
0.80	0.047	15.777	-13.836	12.480	-9.105	9.771
0.90	-0.101	34.606	-17.207	18.341	-12.593	13.444

Table 3

Major descriptive statistics of BEA and of all the forcings (logged values when applicable)*.(a) list, (b) volatility, (c) ADF stationary/nonstationary test result (S/N) within 5% *p*-value, (d) estimated *p*-value of ADF test, (e) achieved min/max date.

a	b	c	d	e	a	b		d	e
BEA	0.0681	S	0.0071	1911 / 1998	AEROSOL	-0.9009	N	0.6820	2006 / 1850
SUNSPOTS	0.2838	S	0.0010	1913 / 1957	AERF	-0.9024	N	0.7681	2006 / 1850
SOL	-0.3556	S	0.0137	1888 / 1989	FCO2	0.0133	N	0.9990	1850 / 2006
SIR	0.0000	S	0.0010	1902 / 1981	FCH4	0.0371	N	0.7203	1850 / 2003
TSI	0.0000	S	0.0012	1923 / 1958	FN2O	0.0035	N	0.9990	1850 / 2006
VOLSOL	-0.3768	S	0.0010	1855 / 1993	VOL	-2.1790	S	0.0010	1992 / 1850
COMPSOL	-0.4328	S	0.0010	1973 / 1884	COMPVOL	-0.4411	S	0.0010	1972 / 1983
CRI	0.0373	S	0.0010	1990 / 1903	PDO	-7.4803	S	0.0010	1917 / 1983
C14RLS	0.7885	S	0.0010	1888 / 1989	NAOM	3.7261	S	0.0010	1965 / 2000
C14BLS	0.8964	S	0.0010	1888 / 1989	GSULFEM	0.1315	N	0.9572	1850 / 1980
BE10BS	-0.4411	S	0.0135	1887 / 1989	CO2	0.9123	N	0.9990	1854 / 2006
BE10LS	-0.3613	S	0.0111	1888 / 1989	CH4	0.9286	N	0.5988	1850 / 2006
CO2V	0.2063	N	0.3619	1850 / 2006	N2O	0.9914	N	0.9990	1850 / 2006
CO2RF	-1.8603	N	0.9562	1850 / 2006	CFC11	1.6671	S	0.0397	1850 / 1987
INCOME_E	0.0934	N	0.5434	1860 / 2006	CFC12	1.6936	S	0.0052	1850 / 2001
INCOME_O	0.0921	S	0.0282	1850 / 2006	SOX	-0.7578	N	0.9261	1989 / 1850
POP_E	0.0203	N	0.9222	1850 / 2006	VOLGL	-1.6816	S	0.0010	1885 / 1853
POP_O	0.0618	N	0.3385	1850 / 2006	SOLS	16.7111	S	0.0010	1889 / 1981
GHG	-1.8748	N	0.9888	1850 / 2006	VOLER	3.2062	S	0.0010	1850 / 1861

* The variables listed are contained in the Section entitled Data Description and Sources. Volatility is measured by the ratio of the mean and the standard deviation.

Table 4

Major results, of alternative GMM models, ranging from two to eight regressor forcings (Sect. 3.2).

List of forcings for each specification model

1)	PDO, SUNSPOTS
2)	PDO, SUNSPOTS, VOL
3)	PDO, SUNSPOTS, VOL, VOLGL
4)	PDO, SUNSPOTS, VOL, VOLGL, VOLER
5)	PDO, SUNSPOTS, VOL, VOLGL, VOLER, COMPVOL
6)	PDO, SUNSPOTS, VOL, VOLGL, VOLER, COMPVOL, VOLSOL
7)	PDO, SUNSPOTS, VOL, VOLGL, VOLER, COMPVOL, VOLSOL, COMPSOL

A. True number of factors (col. 1) and of instruments (col.2) — B. Selected nominal factor shares

1)	2	4	0.3014	0.2411	0.2111						
2)	3	6	0.3014	0.2411	0.2111	0.0789					
3)	4	8	0.3014	0.2411	0.2111	0.0789	0.0524				
4)	5	10	0.3014	0.2411	0.2111	0.0789	0.0524	0.0452			
5)	6	12	0.3014	0.2411	0.2111	0.0789	0.0524	0.0452	0.0411		
6)	7	14	0.3014	0.2411	0.2111	0.0789	0.0524	0.0452	0.0411	0.0129	
7)	8	16	0.3014	0.2411	0.2111	0.0789	0.0524	0.0452	0.0411	0.0129	0.0114

C. Endogeneity tests: Granger causality F stats running from structural residuals to forcings and viceversa, and critical values

1)	2.5470	4.6404	3.9055				
1)	2.5905	0.8930	3.9055				
2)	2.6760	4.7543	0.0008	3.9051			
2)	2.0389	0.2316	2.8499	3.9051			
3)	2.7304	4.6920	0.0091	0.4184	3.9051		
3)	2.6523	0.1518	1.2386	1.1994	3.9051		
4)	2.6620	4.2898	0.0274	0.1472	1.0852	3.9051	
4)	2.3198	0.0857	1.0547	0.7630	0.2080	3.9051	
5)	2.5773	4.6410	0.0030	0.1451	4.2606	1.1638	2.6666
5)	2.8351	0.1595	1.1485	0.9056	0.5153	5.4783	2.6666

6)	2.6878	5.0267	0.0025	0.1351	4.2160	1.2034	2.0958	2.6666	
6)	2.3824	0.2686	0.4855	0.6797	0.2622	5.5313	4.9829	2.6666	
7)	2.6528	5.0900	0.0064	0.1491	4.1555	1.2107	1.8705	3.1756	3.9051
7)	2.7524	0.4073	0.4882	0.9860	0.1419	5.6389	4.6097	0.4164	3.9051

D. TSLS WI tests for vector $\beta = 0$: AR, LM, LR and respective *p*-values

1)	2.4305	0.6572	0.6587
1)	0.6571	0.4176	0.4170
2)	5.7380	1.3178	1.3222
2)	0.4532	0.2510	0.2502
3)	7.6988	2.3244	2.3268
3)	0.4634	0.1274	0.1272
4)	13.9625	10.9456	10.9505
4)	0.1747	0.0009	0.0009
5)	13.9758	10.7394	10.7409
5)	0.3023	0.0010	0.0010
6)	16.0940	11.6492	11.6505
6)	0.3077	0.0006	0.0006
7)	17.4930	10.5583	10.5587
7)	0.3544	0.0012	0.0012

	E. Relevance tests: Minimum eigenvalues of Concentration Parameter and Cragg-Donald		F. Joint exogeneity and relevance tests: Qiv, AR and asymptotic AR for TSLS		
1)	27.8404	696.1180	23.1332	1.6404	0.6930
2)	27.6985	509.0470	21.0896	3.9022	1.5900
3)	26.7769	385.6488	19.7067	4.9059	2.6496
4)	22.4131	263.3865	19.9415	1.7154	3.8104
5)	21.3671	210.6452	19.2356	1.9079	5.0410
6)	16.9785	143.2601	14.7253	2.7493	6.3224
7)	16.9382	124.2185	12.5445	4.9634	7.6426

G. GMM standard and asymptotic J statistics (N,0,1) and respective *p*-values

H. GMM standard and asymptotic AR statistics (N,0,2) and respective *p*-values

1)	1.8940	0.5947	-1.1853	0.8820	1.8432	0.9335	-1.6970	0.8019
2)	4.4257	0.3515	-0.8936	0.8142	4.3206	0.8271	-1.3009	0.7423
3)	5.1139	0.4021	-1.0926	0.8627	4.9472	0.8947	-1.5978	0.7878
4)	1.9913	0.9205	-2.0430	0.9795	1.8610	0.9996	-2.9269	0.9283
5)	2.2238	0.9464	-2.2255	0.9870	2.0524	0.9999	-3.1931	0.9448
6)	2.9816	0.9355	-2.3014	0.9893	2.7263	0.9999	-3.3184	0.9515
7)	5.7299	0.7666	-2.0450	0.9796	5.2589	0.9984	-3.0031	0.9334

I. GMM key statistics: Standard Error, Durbin Watson, ARCH(1), ARCH(1) p-value, and Autocorrelation(1) coefficient

1)	0.0056	2.0251	0.1963	0.6577	-0.0138
2)	0.0056	2.0392	0.2176	0.6409	-0.0209
3)	0.0056	2.0835	0.3567	0.5503	-0.0437
4)	0.0060	2.1007	1.5482	0.2134	-0.0527
5)	0.0062	2.0993	1.0838	0.2979	-0.0515
6)	0.0061	2.0753	1.1227	0.2893	-0.0411
7)	0.0057	2.1048	1.9268	0.1651	-0.0553

J. GMM coefficient vector and t statistics

1)	-0.0011	0.0011						
1)	-0.6387	1.4098						
2)	-0.0013	0.0011	0.0006					
2)	-1.0899	0.8707	0.2515					
3)	-0.0017	0.0002	0.0012	0.0011				
3)	-1.8989	0.1512	0.4706	0.6557				
4)	-0.0014	0.0017	0.0013	0.0009	0.0112			
4)	-1.1093	1.7678	0.9884	0.6642	3.9752			
5)	-0.0018	0.0015	0.0006	-0.0017	0.0082	-0.0038		
5)	-1.1467	1.6388	0.2521	-0.6775	4.9233	-1.9056		
6)	-0.0027	0.0018	-0.0007	-0.0012	0.0053	-0.0028	-0.0046	
6)	-2.3796	2.4764	-0.5209	-0.7644	4.0221	-1.6423	-2.2653	
7)	-0.0014	0.0009	0.0007	-0.0002	0.0051	-0.0026	-0.0042	-0.0011
7)	-1.0109	1.0616	0.3838	-0.1526	3.3978	-1.4467	-2.5303	-0.3243

K. Kleibergen GMM tests for vector $\beta = 0$: values and p-values (p) of Jacobian rank (RK), Wald (W), S, KLM, JKLM and MQLR statistics

	RK	RK p	W	W p	S	S p
1)	64.714	0	0.0465	0.9974	8.807	0.0661
2)	22.460	0	0.0709	0.9994	11.294	0.0797
3)	20.251	0	0.1859	0.9993	13.800	0.0871
4)	208.143	0	3.257	0.7760	27.736	0.0020
5)	101.640	0	11.581	0.1152	54.818	0.0020
6)	137.583	0	5.608	0.6911	64.114	0
7)	152.325	0	0.4584	1.0000	73.489	0

	KLM	KLM p	JKLM	JKLM p	MQLR	MQLR p
1)	6.092	0.1072	2.715	0.0994	6.334	0.0891
2)	7.749	0.1012	3.545	0.1699	8.742	0.0518
3)	9.893	0.0783	3.908	0.2716	11.291	0.0347
4)	19.126	0.0040	8.610	0.0716	19.877	0.0022
5)	49.486	0.0040	5.333	0.3767	51.274	0
6)	54.533	0	9.581	0.1434	57.352	0
7)	59.246	0	14.243	0.0470	63.434	0

Table 5

Coefficients, t statistics and shares of selected static GMM model specification*.

Forcings	PDO	SUNSPOTS	VOL	VOLGL	VOLER	COMPVOL	VOLSOL
Coefficients	-0.0027	0.0018	-0.0007	-0.0012	0.0053	-0.0028	-0.0046
t statistics	-2.3796	2.4764	-0.5209	-0.7644	4.0221	-1.6423	-2.2653
Nominal shares	0.3014	0.2411	0.2111	0.0789	0.0524	0.0452	0.0411
Weighted shares	0.3851	0.3205	0.0590	0.0324	0.1132	0.0399	0.0500

* Figures in the first two rows derive from line (6), panel J, Table 4. Figures in the third row derive from line (6), panel B. Figures in the last row are obtained by multiplying the second by the third row and then reweighting.

Figure 1a.
North Atlantic Oscillation Mode (NAOM), years 831−2007.

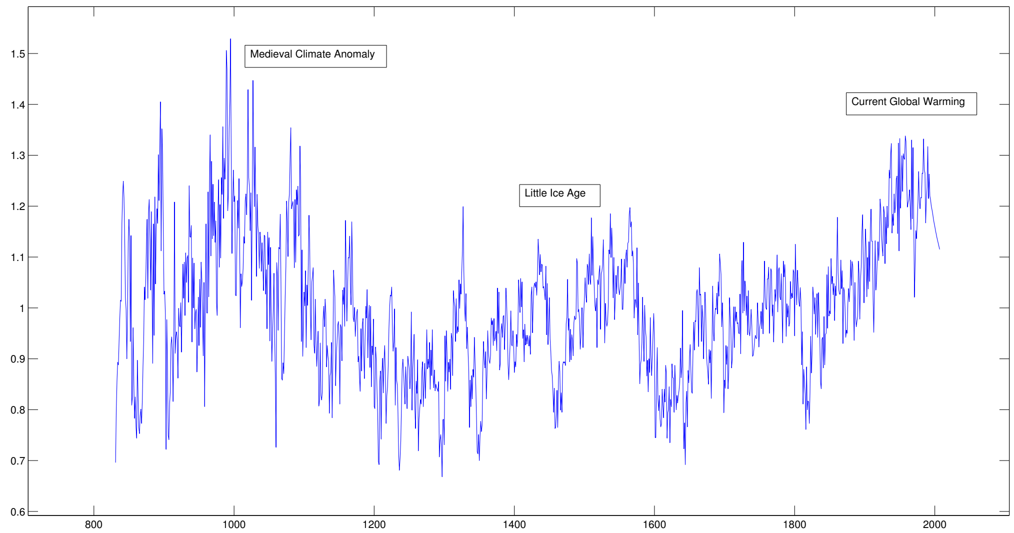

Figure 1b.
Time series of mean World temperatures (BEA), 1850−2006.

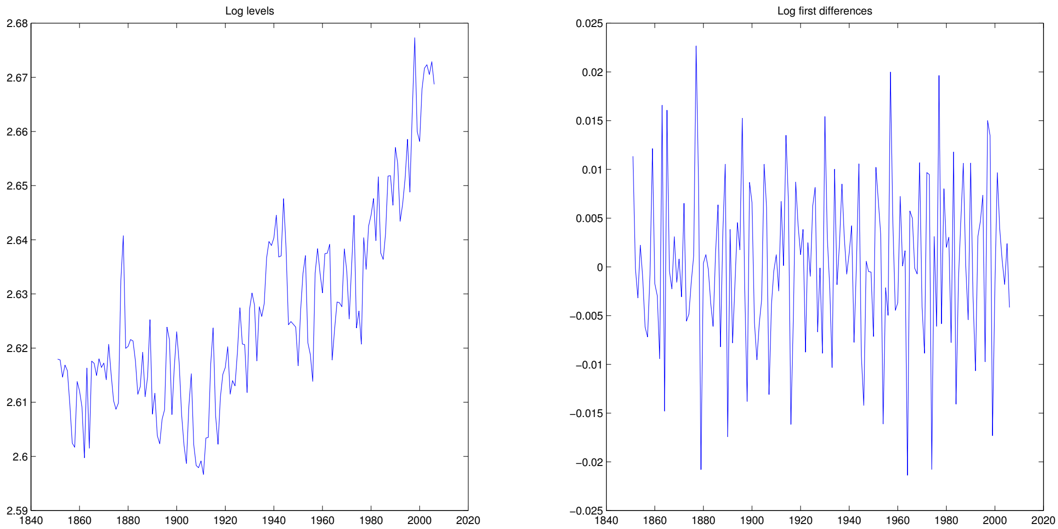

Figure 2a.
Time series of forcings, 1850–2006.

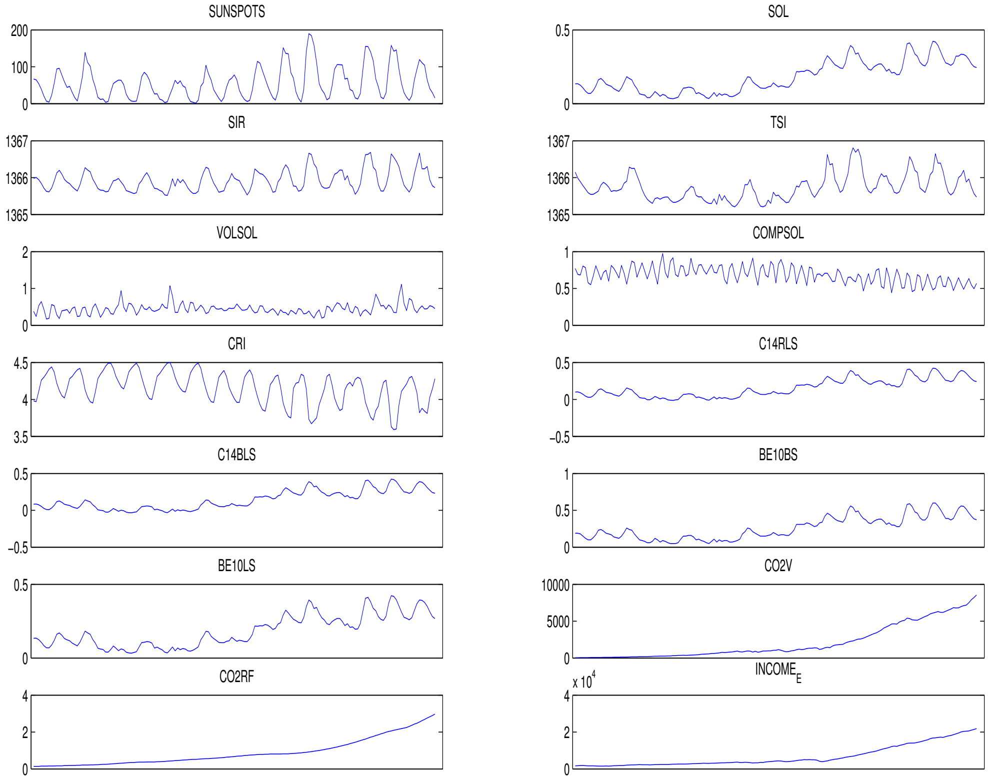

Figure 2b.
Time series of forcings cont., 1850–2006.

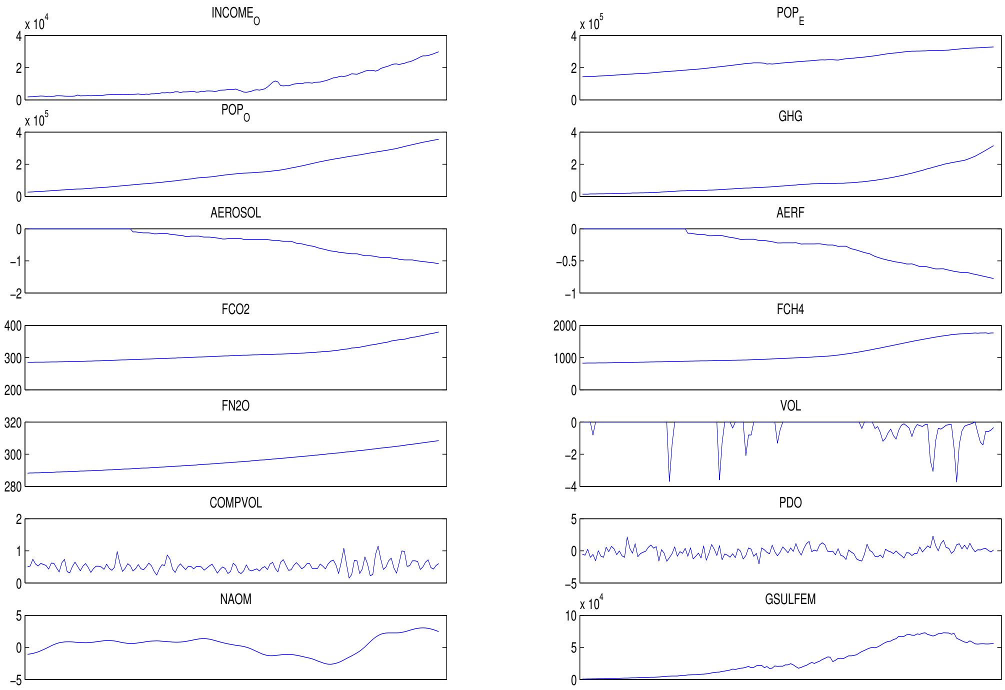

Figure 2c.
Time series of forcings cont., 1850−2006.

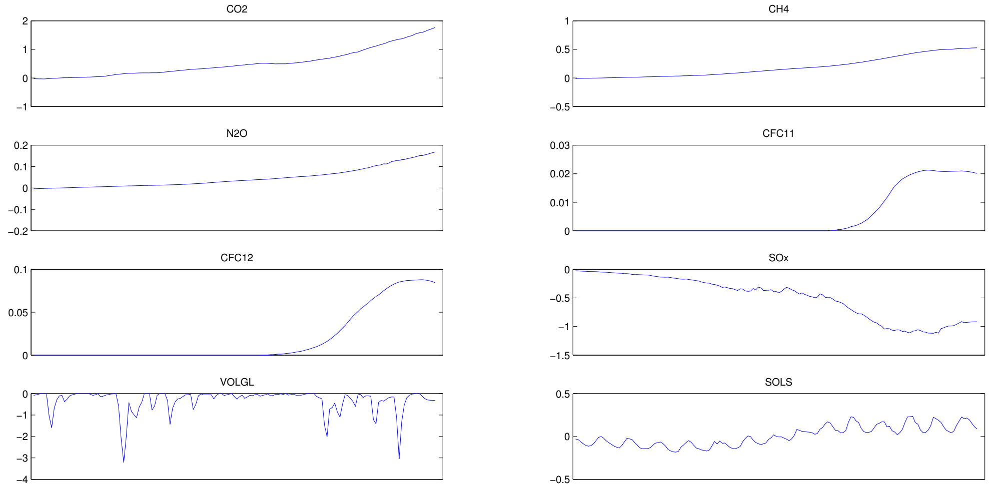

Figure 3.
Estimated time series of t−statistics of breaks, 1865−2000.

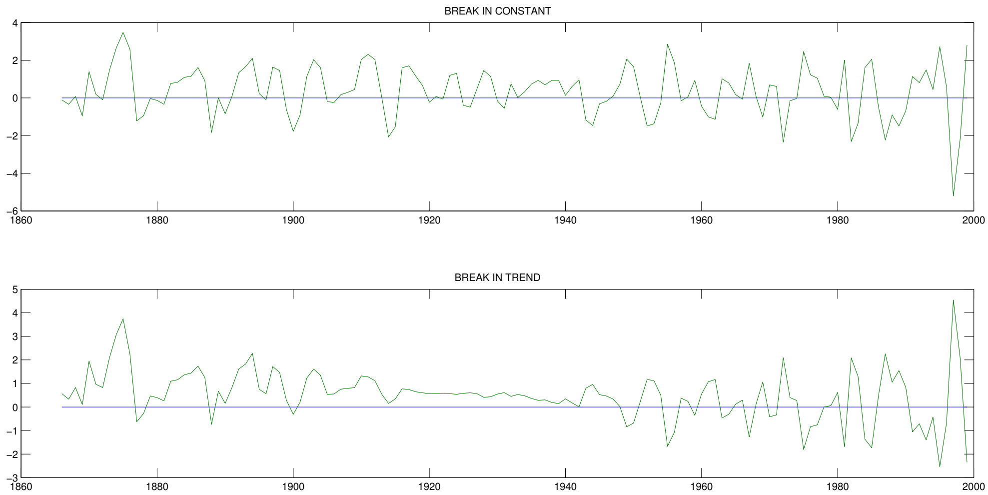

Figure 4.
Estimated time series of forcings weighted shares, 1865−2000.